Modeling cerebral development *in vitro* with L-*MYC*-immortalized human neural stem cell-derived organoids

Alejandra Velazquez Ojeda[1], Dina Awabdeh[1], Blake Brewster[1], Russell Rockne[2], Denis O'Meally[3], Hongwei Holly Yin[4], Nadia Carlesso[1], Christine E. Brown[5], Margarita Gutova[1]*, and Michael E. Barish[1]*

*Co-senior authors.

Departments of
[1]Stem Cell Biology & Regenerative Medicine
[2]Computational & Quantitative Medicine
[3]Diabetes & Cancer Discovery
[4]Cancer Biology & Molecular Medicine
[5]Hematology & Hematopoietic Cell Transplantation
Beckman Research Institute and National Medical Center, City of Hope, Duarte CA 91010

Corresponding author/Lead contact:
Michael E. Barish, Ph.D.
Department of Stem Cell Biology & Regenerative Medicine
Beckman Research Institute, City of Hope
Duarte, CA 91010, USA
Tel: 626/218-8188
E-mail: mbarish@coh.org

Running Title: Immortalized human neural stem cell-derived organoids

Keywords: Human neural stem cells; LMNSC01 cells; NSC-derived organoids; neural lineage differentiation

31   **SUMMARY**

32   E*x vivo* studies of human brain development has been advanced by adoption of organoids recapitulating

33   to varying extents *in utero* patterns of tissue development and cell differentiation. We here present an

34   organoid-based human cortical development platform employing immortalized fetal neural stem cells

35   (LMNSC01) grown in a physiological (4% oxygen) environment. Characterizing LMNSC01 organoids

36   for over 120 days *in vitro* by immunofluorescence and expression profiling (using NanoString), and then

37   comparing these profiles to those of normal cortical development (BrainSpan database), revealed similar

38   developmental patterns for neurons, astrocytes and oligodendrocytes. Notable properties of this platform

39   are its initiation with immortalized authentic human NSCs, growth at physiological oxygen concentration,

40   and subsequent favorable comparison of their gene expression patterns with those observed during

41   cortical development.

42

ABSTRACT

A promising advance for *ex vivo* studies of human brain development and formulation of therapeutic strategies has been the adoption of brain organoids that, to a greater extent than monolayer or spheroid cultures, recapitulate to varying extents the patterns of tissue development and cell differentiation of human brain. Previously, such studies been hampered by limited access to relevant human tissue, inadequate human *in vitro* models, and the necessity of using rodent models that imperfectly reproduce human brain physiology. Here we present a novel organoid-based research platform utilizing L-*MYC*-immortalized human fetal neural stem cells (LMNSC01) grown in a physiological 4% oxygen environment.

We visualized developmental processes in LMNSC01 brain organoids for over 120 days *in vitro* by immunofluorescence and NanoString gene expression profiling. Gene expression patterns revealed by NanoString profiling were quantitatively compared to those occurring during normal brain development (BrainSpan database) using the *Singscore* method. We observe similar developmental patterns in LMNSC01 organoids and developing cortex for genes characterizing neurons, astrocytes, and oligodendrocytes, and multiple pathways including those involved in apoptosis, neuronal cytoskeleton, neurotransmission, and metabolism. Notable properties of this LMNSC01 platform are its initiation with immortalized authentic human neural stem cells, growth in a physiological oxygen environment, the consistency of the organoids produced, and favorable comparison of their gene expression patterns with those reported for normal cortical development.

63 **INTRODUCTION**

64 Brain organoids comprised of human cells recapitulating patterns of cell differentiation and

65 morphological development characteristic of human brain [1-3] to a greater extent than monolayer or

66 spheroid cultures are a powerful platform for *ex vivo* experimentation [2,4,5].

67 We here present a novel organoid platform based on L-*MYC*-immortalized fetal human neural stem cells:

68 LMNSC01[6,7]. These cells can be expanded to create research cell banks while maintaining a stable genetic

69 background [7]. This report is concerned with a cohort of organoids, initiated with LMNSC01 neural stem

70 cells and grown at physiological (4%) oxygen concentrations, that survive for more than four months

71 without signs of necrosis. We observe by immunofluorescence and confocal microscopy emergence of

72 morphologically distinct cells of multiple neural lineages (neuron, astrocyte, oligodendrocyte) expressing

73 differentiation markers indicating cortical/telencephalon identity. At the same time, populations of SOX2-

74 expressing neural progenitor cells are maintained with no evidence of uncontrolled proliferation.

75 We validated this LMNSC01 organoid platform by profiling gene expression in developing organoids (by

76 NanoString), and determining quantitatively (by *Singscore* method) that these patterns compare favorably

77 to those described for developing human brain (BrainSpan database). We also demonstrated organoid-to-

78 organoid reproducibility by observing correlated expression of gene panels in individual organoids of the

79 same age, and separation from those of different ages.

80 Developing platforms for *ex vivo* studies of human brain development and formulation of therapeutic

81 strategies for brain disorders has been hampered by limited access to human brain tissue, inadequate *in*

82 *vitro* models of developing human brain, and use of rodent models that imperfectly recapitulate human

83 brain physiology [8,9]. We suggest that LMNSC01 organoids provide a physiologically relevant and

84 consistent platform for examining regulation of cortical development and function.

85

RESULTS

LMNSC01 organoids exhibit consistent growth and gene expression patterns.

Differentiation of LMNSC01 cells into multiple types of neural lineage cells (i.e., neurons, astrocytes and oligodendrocytes) was originally described in monolayer culture[6], and, here, in organoid cultures. Matrigel-imbedded LMNSC01 cells are grown as free-floating organoids in a 4% O_2 environment approximating that present in fetal brain using characterized NeuroCult Proliferation medium. Over a 1- to 3-month period, LMNSC01 cells within the organoids, differentiate into cells expressing markers of maturing and mature neurons including cortical and hippocampal fated cells, radial glia, astrocytes, and oligodendrocytes, as well as endothelial cells. These organoids are most properly termed "guided" in that they are grown in a medium favoring proliferation (but not otherwise directive), and "telencephalic" based on their tissue of origin[10].

In free-floating LMNSC01 organoids, as illustrated in the brightfield images in **Figure 1A**, the neural stem cells initially proliferate to fill the space delimited by the Matrigel droplet (D0, D15), and then continue to expand, developing internal structure and in some cases distorting the spherical structure of the early organoids (D33, D47). This progression of organoid internal structure is also illustrated in **Figure 1B** using eGFP-expressing LMNSC01 cells. At D15 the NSCs appear distributed relatively homogeneously throughout the organoid, with a more complex internal structure evident at D30. An increasingly complex organization is evident at D60 and is maintained at D90, a self-organization promoted by the supporting Matrigel extracellular matrix.

Over the first 120 days in culture, numbers of cells per organoid show rapid increase over the first 30 days, exhibit a characteristic dip at D60, and then stabilize at approximately 200,000 cells per organoid by D90-D120 (**Figure 1C**). Ultimately, as illustrated by measures of eccentricity (**Figure 1D**), the majority of organoids (greater than 82% for D30-D90) were smoothly spherical or ovoid, with D15 organoids being the most irregular in form (66% smooth/ovoid). The more spherical or ovoid D15-D60 organoids had relatively stable cross-sectional areas of around 2 mm^2 (**Figure 1E**), with D15-D60 organoids having diameters of 1.6-1.7 mm and D90 organoids being somewhat smaller (1.3 mm). In this organoid system, size and thus differentiation may be constrained by Matrigel drop size [11] rather than oxygen and nutrient exchange. In larger organoids it is thought that cells further than 200-400 μm from the surface do not receive sufficient nutrients through diffusion [12] and healthy tissue can be limited to the organoid surface [2]. However, LMNSC01 organoids survived for more than four months without signs of necrosis.

117 Interrogating expression of genes in the NanoString Tissue Integrity theme (**Supplementary Table S1**)

118 over time (**Figure 1F**), and then ordering them according to expression level on D120, revealed two

119 temporal patterns. In **group i**, expression of these genes was similar at D34 and ceased by D120, while

120 expression of genes in **group ii** started at higher levels than those in **group i**, were consistently elevated at

121 D120, and increased or decreased over the interval D34-D120. Gene ontology (GO) analysis

122 (**Supplementary Figure S1)** suggests that there was an increase in representation of processes involved

123 in shaping organoid architecture: "localization", "interspecies interaction between organisms",

124 "developmental processes", "locomotion", "multicellular organismal processes".

125 By D30, LMNSC01 organoids formed layers reminiscent of developing human cortex [13], as illustrated in

126 a series of images at increasing depths along an organoid edge (**Figure 1G**). Towards the organoid interior

127 (**panels i, ii**), GFAP-expressing cells mark a subplate-intermediate zone-like area containing radially

128 aligned β-tubulin III neurons (**panels ii, iii**) and a cortical plate-like region (between white lines in **panel**

129 **iii**). Towards the organoid surface, yellow lines demarcate a marginal zone-like region containing

130 circumferential GFAP-expressing glia (**panels i, iv**) and β-tubulin III-expressing neurons (**panels ii, iii**)

131 extending to the organoid surface (**panel iv**). This marginal zone-like pattern of NeuN- and MAP2-

132 expressing neurons internal to GFAP-expressing glial cells is also illustrated in **Figure 1H**. In **Figure 1I**,

133 a subventricular zone-like area of area of PAX6-expressing cells surrounds a cell-free ventricle-like

134 structure.

Cells in LMNSC01 organoids express markers of cortical and hippocampal neural identity.

136 As shown in **Figure 2**, LMNSC01 organoids expressed markers indicative of a telencephalon (cortical

137 and hippocampal) identity. SOX2-expressing stem and progenitor cells were distributed throughout the

138 organoids, decreasing as a percentage of total cells between D15 and D60, and stabilizing at about 80% of

139 cells by D120 (**Figure 2A1, A2**). FoxG1, marking forebrain-fated cortical progenitor cells [14] were found

140 in D30 organoids and less so in organoids at D90 (**Figure 2B**). Wnt receptor Fzd9, marking hippocampal

141 fate [15], was strongly expressed throughout organoid development, even as cell shapes matured (**Figure**

142 **2C**). Finally, transthyretin (TTR), marking choroid plexus fate [16], was also found in D30 organoids

143 (**Figure 2D**). NanoString expression profiling of organoid cell type markers (**Figure 2E**), and

144 consolidated into a dendrogram (**Figure 2F**), indicates the closest relatedness of organoids to cortical

145 tissue, and their distance from other regions.

Cells in LMNSC01 organoids differentiate into multiple types of neural lineage cells.

147 Differentiation of LMNSC01 cells into neurons, astrocytes and oligodendrocytes was originally described

148 in monolayer culture [6]. LMNSC01 cells grown in 3D organoid culture showed robust differentiation into

149   NSC lineages as presented in roughly developmental order in **Figure 3** by immunofluorescence (**Figure**

150   **3B1-E1**), as percentages of total cells (by dissociation and flow cytometry, **Figure 3B2-E2**), by organoid

151   mRNA expression (NanoString, **Figure 3A2-E2**), and comparison to fetal cortical mRNA (BrainSpan,

152   **Figure 3A2-E2**).

153   Expression of transcription factor T-box brain1 (Tbr1) mRNA, marking postmitotic neurons [17] (**Figure**

154   **3A2**), was higher at early times in organoids (NanoString) (D34-D60/65), and fell progressively (D94-

155   D120) as organoids aged. In fetal cortex (BrainSpan), expression was low at W8/9, elevated at W12/13,

156   and then fell over the interval W16/17 to W35/37. Immunofluorescence also indicated Gremlin 1,

157   important for early cortical excitatory neuron development [18], was expressed in the LMNSC01 organoids

158   (not shown).

159   Doublecortin (DCX), a marker of migrating immature neurons, was present throughout organoid

160   development, with, by immunofluorescence, relative numbers of DCX-expressing cells appearing to

161   decrease between D15 and D90 (**Figure 3B1**). At the mRNA level, expression in organoids (NanoString)

162   was elevated at D34, transiently dipped at D60/65, was high at D90, and then declined over the interval

163   D94 to D120. In developing cortex (BrainSpan), expression increased over the interval W8 to W16/17,

164   then declined over the interval W19 to W35/37 (**Figure 3B2**).

165   Expression of β-tubulin III, marking maturing neurons [19] appeared in organoid immunofluorescence

166   images to increase between D15 and D30, decrease somewhat in the D30-D60 interval, and again

167   increase by D120 (**Figure 3C1).** Counts of percent positive cells **(Figure 3C2)** followed a similar pattern,

168   elevated at D30, reduced at D60, and again elevated at D120. The morphology of β-tubulin III-expressing

169   cells varied over time, becoming longer and more extended over the period D30 to D90, (**Figure 3C1**),

170   perhaps reflecting tubulin's role as a cytoskeletal protein. In fetal cortex (BrainSpan), β-tubulin III

171   expression, similar to DCX, increased somewhat from W8 to W16-W17, and then decreased from

172   W24/26 to W35/37 **(Figure 3C2).**

173   MAP2, a neural differentiation marker [20], was also present from the earliest times (**Figure 3D1**). At the

174   mRNA level, (**Figure 3D2**) expression in organoids (NanoString) was biphasic, elevated at D34, reduced

175   at D60/65, transiently increased at D90, and reduced at D94-D120. In developing cortex (BrainSpan)

176   MAP2 expression (BrainSpan) was mixed during W8 to W16/17, and then progressively decreased from

177   W24/26 to W35/37 (**Figure 3D2**).

178   Expression NeuN, a nuclear marker of mature neurons [21], was surprisingly high by immunofluorescence

179   at D15 (**Figure 3E1**) and as a percent of total cells (**Figure 3E2**), appearing to decrease between D30 and

180   D60, recovering by D90, and increasing to D120 (**Figure 3E2**). Fetal cortex NeuN mRNA levels

181   (BrainSpan) increased from W8 to W16, paused from W17 to W26, and then increased until W35/37,

182   ending the fetal period at higher levels (**Figure 3E2**).

183   There were some consistent expression patterns of these neural antigens. In organoids, markers reflecting

184   intermediate stages of neural differentiation (DCX, β-tubulin III, MAP2) all showed a dip [by cell counts

185   and mRNA (by NanoString)] centered on D60, which is also the time of slower organoid growth as

186   illustrated in **Figure 1C,** before recovering around D90 and, for the mRNA measurements (NanoString),

187   decreasing again at D120. In fetal cortex (BrainSpan), expression of these same three markers described

188   an inverted-U, lower at W8/9, a local maximum at W16 to W20, and then reduction by W35/37. The

189   earliest and latest developmental markers, Tbr1 and NeuN, exhibited reciprocal behaviors. Tbr1 [17] was

190   expressed in organoids (NanoString) initially elevated at D30-D60 and lower at D120. Similarly, in fetal

191   cortex (BrainSpan), Tbr1 expression was higher at W16 and lower by W35-W37. NeuN, marking later

192   stages of neural maturation [21], was in organoids (by cell counts) initially high at D15 (a possible

193   indication of precocious maturation), showed the characteristic dip at D60-D90, before increasing by

194   D120. In fetal cortex NeuN expression (BrainSpan) was reduced at W8/9, increased to W16, stabilized

195   between W17-W26, and then was elevated by W35/37.

196   LMNSC01 organoids also incorporate macroglia: astrocytes and oligodendrocytes. As illustrated in

197   **Figure 4**, SOX9, a transcription factor expressed by neural progenitor cells and by astrocytes in adult

198   brain [22], is found in D30-D60 organoids by immunofluorescence, most notably in the nuclei of vimentin-

199   expressing cells (**Figure 4A, Dai-iii**). For oligodendrocytes, immunofluorescence shows expression of

200   maturing oligodendrocyte marker O1 from D30 to D60 in organoids **(Figure 4B)**. Phosphorylated

201   vimentin, a marker of mitotic astroglial cells [23], was present in cell bodies, showed an increase in

202   expression from D15 to D30 and then declined by D90 (**Figure 4C**). The astrocytic cytoskeletal marker

203   GFAP was present in organoids through the entire culture period to D120, with cells appearing more

204   fibrous at later times (**Figure 4Daiv-vi)**

205   Patterns of GFAP expression in organoids, assessed as percent GFAP^{POS} cells (by flow cytometry) and as

206   mRNA levels (by NanoString) were essentially parallel (**Figure 4Db**), showing increase through D30 to

207   D60, a dip at D90, and an increase at D120. We also observed reciprocal maturation patterns of

208   expression of the progenitor marker SOX9 and the more mature marker GFAP in both organoids (by

209   NanoString) and fetal cortex (by BrainSpan) (**Figure 4Dc,4Dd).** Reciprocal expression of genes

210   characteristic of immature and mature cell states has been noted in other brain organoid studies. For

211   example, Lancaster et al. (2013) observed neuronal differentiation (increase in DCX^{POS} cells) at the

212   expense of SOX2^{POS} progenitors in microcephaly models [2].

213   **LMNSC01-derived organoids express mesodermal markers of endothelial cells and of microglia.**

214   As illustrated in **Figure 5**, we noted intrinsic expression of endothelial markers CD31 (PECAM-1) and

215   von Willebrand Factor (vWF), as well as tight junction marker ZO-1, in organoids created with only

216   LMNSC01 cells. This apparent appearance of mesodermal lineage cells was noted as early as D15. While

217   expression of these markers was less organized at D15, in older organoids (D30, D90) they tended to be

218   seen together and could be observed coalescing in linear arrangements reminiscent of nascent vasculature

219   (yellow arrowheads in **Figure 5**). This immunochemistry was consistent with expression of the individual

220   mRNAs comprising the NanoString endothelial pathway throughout organoid development, declining

221   somewhat in older D120 organoids as well as in the aggregate *Singscore* (**Supplemental Figure S2**).

222   Expression of these same genes was also evident in developing cortex (BrainSpan) (**Supplemental**

223   **Figure S2**), the increases at later times possibly relating to endothelial cell invasion during cortical

224   vascularization [24].

225   Emergence of vascular-like structures may not be unexpected. Human vasculature is formed using soluble

226   factor- and contact-dependent interactions between neural stem cells and endothelial cells [25], conditions

227   that could arise in the organoids. Additionally, apparent direct transdifferentiation of neural stem cells to

228   endothelial-like cells has been reported [26]. Gliobastoma cells also directly undergo apparent endothelial

229   transdifferentiation *in vitro* and in *in vivo* xengraft models [27].

230   mRNA markers of microglia were also present in LMNSC01 organoids (by NanoString) (**Supplemental**

231   **Figure S2**), an unexpected observation given their mesodermal origin in yolk sac erythromyeloid

232   progenitors [28]. The low abundance of microglia in developing cortex (0.5-1% of cells compared to 10% of

233   cells in mature brain) appears reflected in the low mRNA expression of marker genes in developing

234   cortex (BrainSpan) as compared to the organoids (NanoString) (**Supplemental Figure S2**). Similar

235   intrinsic differentiation of microglia in cortical organoids was observed by Ormel et al [29], as was

236   appearance of mesodermal progenitors [30].

Temporal progression of developmental programs in organoids compares favorably to fetal cortical development.

239   As presented in **Figure 6**, we used bulk RNA expression profiling to examine developmental programs in

240   organoids over time in culture [31]. Shown in **Figure 6A1** is cross correlation for expression of the genes in

241   the NanoString Neuroinflammation panel (**Supplemental Table S1**) by each of 33 organoids ranging

242   from D34 to D120 in culture. Evident are consistent high correlations between organoids of the same

243   ages, and sharp demarcations between organoids at other ages, an indication of stable *in vitro*

244   development distinguished by time in culture. **Figure 6A2** shows a similar cross correlation for the same

245   genes during normal fetal development (BrainSpan). As with the organoids, but not as dramatically,

246   expression of the gene set in cortex was consistent with developmental timing.

247   As presented in **Supplemental Table S1,** NanoString organizes genes into six fundamental themes, 24

248   pathways, and five cell types**.** To facilitate direct comparison of *in vitro* and *in vivo* development, we

249   normalized both sets of data to the NanoString internal reference genes (**Supplemental Table S1)**, with

250   *Singscore* values centered on 0.5 indicating deviation from these reference genes as generated by the

251   *Singscore* algorithm [32]. *Singscore* values for several examples of cell types and developmental themes of

252   particular interest are shown in **Figures 6B** and **6C**; the complete set of comparisons is presented in

253   **Supplemental Figure S2**. Evident is that for neurons, astrocytes and oligodendrocytes, expression levels

254   (relative to reference genes) and the velocity of changes for organoids between D34 and D120 (red), and

255   fetal brain between W8 and W37 after conception (black), appear very similar. We examined this concept

256   more explicitly by constructing proportional time scales between 0.0 and 1.0 in which the day of organoid

257   initiation and the day of conception were time 0.0, and the oldest organoids we examined (120 days), and

258   37 weeks post conception (close to the 40 weeks of normal gestation in humans) were time 1.0. In this

259   scheme, the data could be remarkably similar, as indicated in the overlays of these curves, suggesting that

260   for many processes, development of LMNSC01 cells in organoids was paralleling the normal human

261   progression in cortex.

262

DISCUSSION

Here, we present an organoid platform of *in vitro* telencephalon development formed from human fetal neural stem cells (NSCs) immortalized by expression of L-*MYC*. This organoid platform differs from the most commonly used brain organoids in that they employ human NSCs grown in a 4% O_2 environment that more faithfully reproduces the *in vivo* context of developing human cortex [33]. In contrast, most brain organoids are grown in ambient room air with 20% O_2 present, or, rarely, in high-oxygen environments (40%) [34]. Growth in the elevated O_2 concentration of room air may have consequences for organoid development, as the more physiological 4% O_2, similar to O_2 levels of 1-5% reported for developing brain [33], favors self-renewal and neurogenic potential through activation of Wnt signaling pathways [33,35]. It is only the severe hypoxia associated with ischemia (less than 1% O_2) that results in brain damage [33].

The LMNSC01 cells employed here are well-characterized for NSC lineage differentiation [6,7]. Organoids derived using LMNSC01 cells displayed reproducible patterns of proliferation, identity, and associated structural organization, for over 100 days in culture, and survived for more than four months without signs of necrosis. By immunochemistry and bulk RNA expression profiling we were able to assess the cellular compositions of individual organoids [36], and demonstrate gene expression patterns unique to organoid age (**Figure 6A**), an indication of coordinated developmental progression over time. The consistent reproducibility of these organoids is an important factor in achieving the full utility of this platform [37-39].

Transcriptome analysis by NanoString showed time-dependent changes in RNA expression patterns for genes characterizing neurons, astrocytes, and oligodendrocytes, as well as generalized developmental processes, that compared favorably, both quantitatively and temporally, to those seen in human cortex during fetal development, especially at early times (**Figure 6B, 6C**, **Supplemental Figure S2**). Camp et al [40] also noted similarities between gene expression patterns of organoids and normal fetal development, reflecting a consensus that iPSC-derived organoids reflect cortical development as we concluded here for the LMNSC01 organoids.

Nevertheless, establishing human brain organoids directly from NSCs obviates some of the challenges that have emerged when employing embryonic stem cells (ESCs) or induced pluripotent stem cells (iPSCs) as starting materials. These include, depending on the protocol and on the desired neural cell type, potentially months to achieve iPSC reprogramming [41,42], as well as incomplete or erroneous reprogramming [43], possibly related to cell of origin [44], resulting in defects in DNA methylation, chromatin regulation, protein synthesis [45], poor or incomplete differentiation [4,45-49], as well as accumulating somatic mutations [50] resulting in organoid heterogeneity [51,52] that compromise their ultimate utility [37].

295 The human NSC line utilized here (LMNSC01) reflects the normal phenotype of NSCs at their time of

296 immortalization (12 weeks of gestation)[6], rather than of adult NSCs as seen for granule cells of the

297 hippocampal dentate gyrus or the progenitor cells in the rostral migratory stream. As such, they may not

298 appear as versatile as the induced pluripotent stem cells (iPSCs) that have emerged as a source of neural

299 stem or progenitor cells (NSCs or NPCs) used to establish brain organoid cultures using cells from

300 patients with inborn genetic neurological and other conditions [42,53,54]. However, preliminary studies from

301 others have demonstrated that gene editing techniques can introduce precise changes in genetic makeup of

302 NSCs underlying these disorders [55-57]. Taken together with their stability, these studies suggest LMNSC01

303 organoids as an alternative approach to establishing models of inborn brain diseases.

304 The consistency and reproducibility of LMNSC01 organoids, together with their recapitulation of fetal

305 expression patterns, provide the opportunity to observe and control the development and differentiation of

306 multiple neural-lineage cell types within a controlled culture system, assess the impact of environmental

307 perturbations on these processes, as well as serve as a platform for drug and therapy screening. Further,

308 their chromosomal stability and the absence of tumorigenicity make these organoids potentially suitable

309 source material for implantation and engraftment therapies.

310 Responses of LMNSC01 organoid to variations in growth conditions further suggest future refinements

311 that more closely following fetal brain development, as seen with, for example, the transition from NC

312 Proliferation medium to NC Differentiation medium after initial periods in culture, as illustrated in **Figure**

313 **7** (see also [2]), where changes in cell development after transition to a differentiating medium at D15 are

314 illustrated (**Figure 7A**). Under this condition, organoids undergo growth arrest without a concomitant

315 reduction in size (**Figure 7B**). By D30, β-tubulin III-expressing neurons (**Figure 7C)** develop varicosities

316 in differentiating medium (**i → ii**) suggesting synaptogenesis, as indicated by expression of synapsin1 in

317 MAP2-expressing neuron processes (**iii**). By D104, GFAP[POS] astrocytic cells (**Figure 7D**) in

318 differentiating medium extend processes and form fascicles not evident when grown in NC Proliferation

319 medium. O1-expressing oligodendrocyte-like cells (**Figure 7E**) in differentiating medium between D30-

320 D104 acquire a ramified morphology also not evident when grown in proliferation medium (compare with

321 **Figure 4B**).

322 Additional refinements could add additional cell types providing a closer relatedness to fetal cortical

323 development. For example, rather than growing progenitors and immature neurons on an initially

324 homogeneous scaffold, introducing structural, cues or providing local presence of additional cell types

325 may shape more physiological spatial arrangements of differentiated cells. Further, apparent *de novo*

326 appearance of endothelial cells and vasculature-like structures, as well as microglial gene expression

327 suggesting development of these cells, raise the possibility that culture conditions could be manipulated to

328   promote appearance of these cell types, thereby providing a more complete cortical model and further

329   enhancing the utility of these organoids [58-60].

330

EXPERIMENTAL PROCEDURES

Resource availability

Further information and requests for resources and reagents should be directed to and will be fulfilled by the lead contact, Michael Barish (mbarish@coh.org).

Expansion of LMNSC01 cells

Fetal brain neural stem cells were obtained from discarded tissue from Advanced Bioscience Resources under a City of Hope Institutional Review Board approved protocol (City of Hope IRB 10079) and L-*MYC* immortalized as described previously [6]. LMNSC01 cells were expanded using a hollow fiber bioreactor (Terumo Quantum Cell Expansion System) in serum-free NSC medium (RHB-A medium; Cell Science) supplemented with growth factors (10 ng/mL bFGF, 10 ng/mL EGF; both from PeproTech), 2 mM L-glutamine (Invitrogen), Gem21 NeuroPlex Serum-Free Supplement (GeminiBio-Products 400-160) and penicillin-streptomycin (Mediatech, 30-002-CI) [61].

Organoid preparation

Prior to organoid assembly, expanded LMNSC01 cells were cultured to 80-90% confluence beginning at 10,000 cells/cm^2 using NeuroCult Proliferation medium (StemCell Technologies 05751) supplemented with EGF (10 ng/mL, PeproTech AF-100-15), FGF (10 ng/mL, PeproTech 100-188), heparin (1 U/mL, (StemCell Technologies 07980), at 37 °C in a 4% O_2, 5% CO_2 environment. This medium was also used to culture the organoids.

Our method for LMNSC01 organoid preparation is modified from those described by Hubert et al [62] and Lancaster et al [63]. Each well of a 6-well plate was prepared by placing a 2.5 × 2.5 cm square of parafilm, sterilizing with 70% ethanol, and placing it uncovered in a culture hood under UV light for approximately 30 min for the ethanol to evaporate. At the same time, 500 μL of growth factor reduced Matrigel (Corning 356231) was placed in a microcentrifuge tube to which 83,000 cells were added and gently mixed. Using a repeating pipettor (Eppendorf 4049-7134), ten 6 μL-droplets/well, each containing 1,000 LMNSC01 cells, were dispensed onto the parafilm, and allowed to polymerize for 3 hours in the 37 °C, 4% O_2, 5% CO_2 incubator. The parafilm inserts were then gently removed, and 4 mL of NeuroCult Proliferation medium supplemented as above was added to each well, into which six LMNSC01/Matrigel droplets were added using a sterile spatula. The culture plate was returned to the 37 °C, 4% O_2, 5% CO_2 incubator for three days, after which the culture plate was transferred to a sterilized orbital shaker maintained in the incubator at 100 rpm. Culture medium was changed once per week for the first three weeks, and then twice per week thereafter. In some cases, LMNSC01 cells were engineered to express lentiviral eGFP and used to create organoids for imaging 3-dimensional organization (Zen 3.6, Zeiss)

Immunostaining and imaging

Organoids were fixed for 30 minutes in 4% paraformaldehyde (PFA) in PBS at room temperature (RT), and then washed three times (3×) for 15 min with Tris-buffered saline (TBS) containing 0.1% Triton X-100 (Tx-100) (TBS wash solution). After washing, samples were permeabilized and blocked for one hour in blocking solution: TBS containing 1% Triton and 5% high avidity bovine serum albumin (BSA). Organoids were then incubated overnight at 4 °C with primary antibodies diluted in the same TBS blocking solution, then washed 3× (15 min each) with TBS wash solution with gentle agitation. Secondary antibodies were then applied in TBS blocking solution and incubated overnight at 4 °C. Organoids were then washed 3× with TBS wash solution and mounted on a glass slide with Prolong Glass (Invitrogen). After at least 48 hr at room temperature in the dark to allow for curing of the Prolong Glass, organoids were imaged using Zeiss LSM-700 or LSM-900 confocal microscopes. Images were processed and analyzed using Zen 3.6 (Zeiss) and Imaris 9 (Oxford Instruments).

Reagents for immunostaining

Primary antibodies used for immunofluorescence: Stem cells: SOX2 (EMD Millipore AB5603, 1:300). Astroglial lineage: GFAP (Abcam ab53554, 1:300); vimentin (Abcam ab8069, 1:200); phospho-vimentin (p-vimentin, Abcam ab22651, 1:700); SOX9 (Novus Biologicals AF3075, 1:100). Oligodendroglial lineage: O1 (ThermoFisher 14-6506-82, 1:300). Neural lineage: Gremlin 1 (Bioss Antibodies bs1475R, 1:100); doublecortin (DCX, Santa Cruz Biotech SC-8066, 1:50); β-tubulin III (Biolegend Tuj1 801202, 1:700); NeuN (Abcam ab104224, 1:150); MAP2 (Abcam ab11267, 1:300). Hippocampal progenitor: Fzd9 (Origene TA340718, 1:300). Cortical progenitor: PAX6 (Biolegend 901301, 1:300); FoxG1 (Abcam ab18259, 1:300). Endothelial differentiation: CD31 (PECAM1, Santa Cruz Biotech SC1506, 1:300); von Willebrand Factor (vWF, Dako A0082, 1:300); ZO-1 (Invitrogen 33-9100, 1:300). Choroid plexus: transthyretin (TTR, Serotec AHP1837, 1:100)..

Secondary antibodies: Donkey anti-rabbit Alexa Fluor 488 (Invitrogen A21206, 1:1000). Donkey anti-mouse Alexa Fluor 555 (Invitrogen A21147, 1:1000); Donkey anti-sheep Alexa Fluor 555 (Invitrogen A21436, 1:1000). Donkey anti-goat Alexa Fluor 647 (Invitrogen A21447, 1:1000). Donkey anti-mouse Alexa Fluor 647 (Invitrogen A31571, 1:1000).

Nuclear stain: Hoechst 33342 (Invitrogen H3570, 1:1000).

Flow cytometry

Organoids were dissociated using Neuron Dissociation Solutions (Fujifilm Wako Pure Chemical 291-78001), consisting of Enzyme Solution (295-78021), Dispersion Solution (298-78011) and Isolation Solution (202-78031), per the manufacturer's instructions, with exceptions that incubation times for each

395 solution were reduced to 3-5 min and organoids were gently agitated 10-20 times between

396 solutions. Following dissociation (pipetted using a 200 µL tip), the 1.5 mL Eppendorf tube containing the

397 dissociated cells was centrifuged for 5 min at 400 × g, the supernatant was removed, cells were

398 resuspended for 15 min in 100 µL PBS on ice, and then centrifuged for 5 min at 400 × g. The supernatant

399 was then removed, cells were resuspended in 100 µL PBS + fixable viability dye eFluor450 (eBioscience

400 65-0863-15, 1:1000) on ice for 15 min, centrifuged for 5 min at 400 × g, the dye solution was removed,

401 and the cells were resuspended in 100 µL Fixing Reagent A (Life Technologies GAS002) for 15 min at

402 room temperature (RT). Cells were then centrifuged for 5 min at 400 × g, the supernatant was removed,

403 10 µL Permeabilizing and Staining Reagent B with antibodies was added. Cells were incubated at RT for

404 15 min, then centrifuged for 5 min at 400 × g. The supernatant was then removed, and the cells washed

405 2× with FACS buffer. Finally, cells were resuspended in 100 µL FACS buffer and run for flow cytometry

406 using a MAQSQuant Analyzer 10 (Miltenyi Biotech). Data were analyzed using FCS Express (DeNovo

407 Software).

Reagents for flow cytometry

409 Antibodies for flow cytometry: NeuN:PE (Novus Biologicals NBP1-92693PE); SOX2:APC (R&D

410 Systems IC2018R-100UG); GFAP:PerCP (Novus Biologicals NBP2-33184PCP); β-tubulin III:PE:Cy7

411 (Biolegend 801218).

412 PerCP isotype control (R&D Systems IC002C). PE isotype control (Invitrogen MG2B04). PE:Cy7

413 isotype control (Biolegend 400232).

414 Compensation beads (Invitrogen 01-3333-42).

NanoString gene expression profiling

416 mRNA expression was analyzed using the nCounter Human Neuropathology Panel (Catalog number: XT-

417 CSO-HNROP1-12, NanoString), by digitally detecting and counting in a single reaction without

418 amplification. The Neuropathology Panel consists of genes targeting six fundamental

419 themes: neurotransmission, neuron-glia interactions, neuroplasticity, cell structure integrity,

420 neuroinflammation, and metabolism (**Supplemental Table S1**). Each assay also includes six positive and

421 eight negative mRNA assay controls, plus ten housekeeping mRNA controls. RNA was hybridized with

422 the gene panel Codeset at 65 °C for 16 hr. The post-hybridization probe-target mixture was quantified

423 using the nCounter Digital Analyzer, with subsequent data analysis performed using nSolver. Raw data

424 were first normalized to internal positive and negative controls to eliminate variability unrelated to the

425 samples, then normalized to the selected housekeeping genes using Geometric Means methods.

426 Housekeeping gene expression variability of less than 20% within a single organoid was the criterion for

427 acceptance.

428 mRNA extraction and preparation for NanoString was done at the COH Pathology Core. Briefly, mRNA

429 was extracted using the RNeasy mini kit (Qiagen HB-1277-066). Concentration was measured by

430 Nanodrop spectrophotometer ND-1000 and Qubit 3.0 Fluorometer (Thermo Scientific), with mRNA

431 fragmentation and quality assessed by 2100 Bioanalyzer (Agilent).

432 NanoString data were compared against a reference database for expression of these same genes during

433 normal cortical development (other brain regions excluded) drawn from the BrainSpan Atlas of the

434 Developing Human Brain (https://www.brainspan.org/). To facilitate comparisons, both organoid and fetal

435 brain datasets were normalized to the expression of the same NanoString internal reference genes

436 (**Supplemental Table S1**) using *Singscore* [32]. *Singscore* ranks gene expression and calculates a non-

437 parametric score for individual genes in each gene set (NanoString or BrainSpan). This rank-based

438 approach is robust to differences in the underlying data distribution, enabling scoring of gene sets across

439 different transcriptomic datasets and assessing gene set activity in individual samples. In the single-

440 sample presentation employed here, scores range between 0.0 and 1.0 and represent the extent to which

441 each gene in the gene set is expressed as compared to the distribution of reference genes, and scored as

442 higher (score > 0.5) or lower (score < 0.5) (**Supplemental Figure S2**).

443 **Statistical comparisons**

444 Tests for statistical significance ($p < 0.05$), and internal correlations of NanoString and BrainSpan data

445 (**Figure 6**), were made using Prism v9 (Graph Pad).

446 **Gene Ontology**

447 Tissue integrity genes presented in **Figure 1F** were interrogated for gene ontology

448 (https://geneontology.org) [64,65] and compared using the "Gene ontology enrichment analysis for biological

449 processes" tool [66].

450

ACKNOWLEDGEMENTS

AUTHOR CONTRIBUTIONS

Conceptualization: A.V.O., M.G., M.E.B.

Methodology: A.V.O., B.B., N.C., M.G., M.E.B.

Software Programming: n/a

Validation: n/a

Formal Analysis: R.R., D.O'M., H.H.Y., M.E.B.

Investigation: A.V.O., D.A.

Resources: C.E.B., M.G.

Data Curation: D.A., B.B., M.E.B.

Writing – Original Draft: A.V.O., D.A. M.E.B.

Writing – Review and Editing: A.V.O., D.A., M.G., M.E.B.

Visualization: A.V.O., D.A., M.E.B.

Supervision: M.G., M.E.B.

Project Administration: n/a

Funding Acquisition: C.E.B., M.G., M.E.B.

DECLARATION OF INTERESTS

REFERENCES

1. Velasco, S., Kedaigle, A.J., Simmons, S.K., Nash, A., Rocha, M., Quadrato, G., Paulsen, B., Nguyen, L., Adiconis, X., Regev, A., et al. (2019). Individual brain organoids reproducibly form cell diversity of the human cerebral cortex. Nature *570*, 523-527. 10.1038/s41586-019-1289-x.

2. Lancaster, M.A., Renner, M., Martin, C.A., Wenzel, D., Bicknell, L.S., Hurles, M.E., Homfray, T., Penninger, J.M., Jackson, A.P., and Knoblich, J.A. (2013). Cerebral organoids model human brain development and microcephaly. Nature *501*, 373-379. 10.1038/nature12517.

3. Albanese, A., Swaney, J.M., Yun, D.H., Evans, N.B., Antonucci, J.M., Velasco, S., Sohn, C.H., Arlotta, P., Gehrke, L., and Chung, K. (2020). Multiscale 3D phenotyping of human cerebral organoids. Sci Rep *10*, 21487. 10.1038/s41598-020-78130-7.

4. Arlotta, P., and Pasca, S.P. (2019). Cell diversity in the human cerebral cortex: from the embryo to brain organoids. Curr Opin Neurobiol *56*, 194-198. 10.1016/j.conb.2019.03.001.

5. Pasca, S.P. (2019). Assembling human brain organoids. Science *363*, 126-127. 10.1126/science.aau5729.

6. Li, Z., Oganesyan, D., Mooney, R., Rong, X., Christensen, M.J., Shahmanyan, D., Perrigue, P.M., Benetatos, J., Tsaturyan, L., Aramburo, S., et al. (2016). L-MYC Expression Maintains Self-Renewal and Prolongs Multipotency of Primary Human Neural Stem Cells. Stem Cell Reports *7*, 483-495. 10.1016/j.stemcr.2016.07.013.

7. Rockne, R.C., Adhikarla, V., Tsaturyan, L., Li, Z., Masihi, M.B., Aboody, K.S., Barish, M.E., and Gutova, M. (2018). Long-term stability and computational analysis of migration patterns of L-MYC immortalized neural stem cells in the brain. PLoS One *13*, e0199967. 10.1371/journal.pone.0199967.

8. Balikov, D.A., Neal, E.H., and Lippmann, E.S. (2019). Organotypic Neurovascular Models: Past Results and Future Directions. Trends Mol Med. 10.1016/j.molmed.2019.09.010.

9. Lopez-Tobon, A., Villa, C.E., Cheroni, C., Trattaro, S., Caporale, N., Conforti, P., Iennaco, R., Lachgar, M., Rigoli, M.T., Marco de la Cruz, B., et al. (2019). Human Cortical Organoids Expose a Differential Function of GSK3 on Cortical Neurogenesis. Stem Cell Reports *13*, 847-861. 10.1016/j.stemcr.2019.09.005.

10. Pasca, S.P., Arlotta, P., Bateup, H.S., Camp, J.G., Cappello, S., Gage, F.H., Knoblich, J.A., Kriegstein, A.R., Lancaster, M.A., Ming, G.L., et al. (2022). A nomenclature consensus for nervous system organoids and assembloids. Nature *609*, 907-910. 10.1038/s41586-022-05219-6.

11. Chiaradia, I., Imaz-Rosshandler, I., Nilges, B.S., Boulanger, J., Pellegrini, L., Das, R., Kashikar, N.D., and Lancaster, M.A. (2023). Tissue morphology influences the temporal program of human brain organoid development. Cell Stem Cell *30*, 1351-1367 e1310. 10.1016/j.stem.2023.09.003.

12. Rambani, K., Vukasinovic, J., Glezer, A., and Potter, S.M. (2009). Culturing thick brain slices: an interstitial 3D microperfusion system for enhanced viability. J Neurosci Methods *180*, 243-254. 10.1016/j.jneumeth.2009.03.016.

13. Bystron, I., Blakemore, C., and Rakic, P. (2008). Development of the human cerebral cortex: Boulder Committee revisited. Nat Rev Neurosci *9*, 110-122. 10.1038/nrn2252.

14. Hou, P.S., hAilin, D.O., Vogel, T., and Hanashima, C. (2020). Transcription and Beyond: Delineating FOXG1 Function in Cortical Development and Disorders. Front Cell Neurosci *14*, 35. 10.3389/fncel.2020.00035.

15. Zhao, C., and Pleasure, S.J. (2004). Frizzled-9 promoter drives expression of transgenes in the medial wall of the cortex and its chief derivative the hippocampus. Genesis *40*, 32-39. 10.1002/gene.20058.

16. Dickson, P.W., and Schreiber, G. (1986). High levels of messenger RNA for transthyretin (prealbumin) in human choroid plexus. Neurosci Lett *66*, 311-315. 10.1016/0304-3940(86)90037-6.

17. Englund, C., Fink, A., Lau, C., Pham, D., Daza, R.A., Bulfone, A., Kowalczyk, T., and Hevner, R.F. (2005). Pax6, Tbr2, and Tbr1 are expressed sequentially by radial glia, intermediate progenitor cells, and postmitotic neurons in developing neocortex. J Neurosci *25*, 247-251. 10.1523/JNEUROSCI.2899-04.2005.

18. Ichinose, M., Suzuki, N., Wang, T., Kobayashi, H., Vrbanac, L., Ng, J.Q., Wright, J.A., Lannagan, T.R.M., Gieniec, K.A., Lewis, M., et al. (2021). The BMP antagonist gremlin 1 contributes to the development of cortical excitatory neurons, motor balance and fear responses. Development *148*. 10.1242/dev.195883.

19. Menezes, J.R., and Luskin, M.B. (1994). Expression of neuron-specific tubulin defines a novel population in the proliferative layers of the developing telencephalon. J Neurosci *14*, 5399-5416. 10.1523/JNEUROSCI.14-09-05399.1994.

20. Soltani, M.H., Pichardo, R., Song, Z., Sangha, N., Camacho, F., Satyamoorthy, K., Sangueza, O.P., and Setaluri, V. (2005). Microtubule-associated protein 2, a marker of neuronal differentiation, induces mitotic defects, inhibits growth of melanoma cells, and predicts metastatic potential of cutaneous melanoma. Am J Pathol *166*, 1841-1850. 10.1016/S0002-9440(10)62493-5.

21. Mullen, R.J., Buck, C.R., and Smith, A.M. (1992). NeuN, a neuronal specific nuclear protein in vertebrates. Development *116*, 201-211. 10.1242/dev.116.1.201.

22. Sun, W., Cornwell, A., Li, J., Peng, S., Osorio, M.J., Aalling, N., Wang, S., Benraiss, A., Lou, N., Goldman, S.A., and Nedergaard, M. (2017). SOX9 Is an Astrocyte-Specific Nuclear Marker in the Adult Brain Outside the Neurogenic Regions. J Neurosci *37*, 4493-4507. 10.1523/JNEUROSCI.3199-16.2017.

23. Chang, I.A., Kwon, K.B., Park, Y.C., and Namgung, U. (2013). Permissive role of Cdc2 activity induced from astrocytes in neurite outgrowth. J Neurochem *125*, 214-224. 10.1111/jnc.12163.

24. Walchli, T., Bisschop, J., Carmeliet, P., Zadeh, G., Monnier, P.P., De Bock, K., and Radovanovic, I. (2023). Shaping the brain vasculature in development and disease in the single-cell era. Nat Rev Neurosci *24*, 271-298. 10.1038/s41583-023-00684-y.

25. Chou, C.H., and Modo, M. (2016). Human neural stem cell-induced endothelial morphogenesis requires autocrine/paracrine and juxtacrine signaling. Sci Rep *6*, 29029. 10.1038/srep29029.

26. Wurmser, A.E., Nakashima, K., Summers, R.G., Toni, N., D'Amour, K.A., Lie, D.C., and Gage, F.H. (2004). Cell fusion-independent differentiation of neural stem cells to the endothelial lineage. Nature *430*, 350-356. 10.1038/nature02604.

27. Soda, Y., Marumoto, T., Friedmann-Morvinski, D., Soda, M., Liu, F., Michiue, H., Pastorino, S., Yang, M., Hoffman, R.M., Kesari, S., and Verma, I.M. (2011). Transdifferentiation of glioblastoma cells into vascular endothelial cells. Proc Natl Acad Sci U S A *108*, 4274-4280. 10.1073/pnas.1016030108.

28. Hattori, Y. (2023). The multifaceted roles of embryonic microglia in the developing brain. Front Cell Neurosci *17*, 988952. 10.3389/fncel.2023.988952.

29. Ormel, P.R., Vieira de Sa, R., van Bodegraven, E.J., Karst, H., Harschnitz, O., Sneeboer, M.A.M., Johansen, L.E., van Dijk, R.E., Scheefhals, N., Berdenis van Berlekom, A., et al. (2018). Microglia innately develop within cerebral organoids. Nat Commun *9*, 4167. 10.1038/s41467-018-06684-2.

30. Quadrato, G., Nguyen, T., Macosko, E.Z., Sherwood, J.L., Min Yang, S., Berger, D.R., Maria, N., Scholvin, J., Goldman, M., Kinney, J.P., et al. (2017). Cell diversity and network dynamics in photosensitive human brain organoids. Nature *545*, 48-53. 10.1038/nature22047.

31. Fleck, J.S., Sanchis-Calleja, F., He, Z., Santel, M., Boyle, M.J., Camp, J.G., and Treutlein, B. (2021). Resolving organoid brain region identities by mapping single-cell genomic data to reference atlases. Cell Stem Cell *28*, 1177-1180. 10.1016/j.stem.2021.03.015.

32. Foroutan, M., Bhuva, D.D., Lyu, R., Horan, K., Cursons, J., and Davis, M.J. (2018). Single sample scoring of molecular phenotypes. BMC Bioinformatics *19*, 404. 10.1186/s12859-018-2435-4.

33. Ortega, J.A., Sirois, C.L., Memi, F., Glidden, N., and Zecevic, N. (2017). Oxygen Levels Regulate the Development of Human Cortical Radial Glia Cells. Cereb Cortex *27*, 3736-3751. 10.1093/cercor/bhw194.

34. Eiraku, M., Watanabe, K., Matsuo-Takasaki, M., Kawada, M., Yonemura, S., Matsumura, M., Wataya, T., Nishiyama, A., Muguruma, K., and Sasai, Y. (2008). Self-organized formation of polarized cortical tissues from ESCs and its active manipulation by extrinsic signals. Cell Stem Cell *3*, 519-532. 10.1016/j.stem.2008.09.002.

35. Dey, D., Shrivastava, V., Joshi, D., Singal, C.M.S., Tyagi, S., Bhat, M.A., Jaiswal, P., Sharma, J.B., Palanichamy, J.K., Sinha, S., et al. (2023). Hypoxia Induces Early Neurogenesis in Human Fetal Neural Stem Cells by Activating the WNT Pathway. Mol Neurobiol *60*, 2910-2921. 10.1007/s12035-023-03248-4.

36. Velasco, S., Paulsen, B., and Arlotta, P. (2020). 3D Brain Organoids: Studying Brain Development and Disease Outside the Embryo. Annu Rev Neurosci *43*, 375-389. 10.1146/annurev-neuro-070918-050154.

37. Quadrato, G., Brown, J., and Arlotta, P. (2016). The promises and challenges of human brain organoids as models of neuropsychiatric disease. Nat Med *22*, 1220-1228. 10.1038/nm.4214.

38. Cable, J., Lutolf, M.P., Fu, J., Park, S.E., Apostolou, A., Chen, S., Song, C.J., Spence, J.R., Liberali, P., Lancaster, M., et al. (2022). Organoids as tools for fundamental discovery and translation-a Keystone Symposia report. Ann N Y Acad Sci *1518*, 196-208. 10.1111/nyas.14874.

39. Sandoval, S.O., Cappuccio, G., Kruth, K., Osenberg, S., Khalil, S.M., Mendez-Albelo, N.M., Padmanabhan, K., Wang, D., Niciu, M.J., Bhattacharyya, A., et al. (2024). Rigor and reproducibility in human brain organoid research: Where we are and where we need to go. Stem Cell Reports *19*, 796-816. 10.1016/j.stemcr.2024.04.008.

40. Camp, J.G., Badsha, F., Florio, M., Kanton, S., Gerber, T., Wilsch-Brauninger, M., Lewitus, E., Sykes, A., Hevers, W., Lancaster, M., et al. (2015). Human cerebral organoids recapitulate gene expression programs of fetal neocortex development. Proc Natl Acad Sci U S A *112*, 15672-15677. 10.1073/pnas.1520760112.

41. Hu, B.Y., Weick, J.P., Yu, J., Ma, L.X., Zhang, X.Q., Thomson, J.A., and Zhang, S.C. (2010). Neural differentiation of human induced pluripotent stem cells follows developmental principles but with variable potency. Proc Natl Acad Sci U S A *107*, 4335-4340. 10.1073/pnas.0910012107.

42. Cerneckis, J., and Shi, Y. (2023). Modeling brain macrophage biology and neurodegenerative diseases using human iPSC-derived neuroimmune organoids. Front Cell Neurosci *17*, 1198715. 10.3389/fncel.2023.1198715.

43. Ohnuki, M., and Takahashi, K. (2015). Present and future challenges of induced pluripotent stem cells. Philos Trans R Soc Lond B Biol Sci *370*, 20140367. 10.1098/rstb.2014.0367.

44. Berghout, C.C., Zevalkink, J., and Hakkaart-Van Roijen, L. (2010). The effects of long-term psychoanalytic treatment on healthcare utilization and work impairment and their associated costs. J Psychiatr Pract *16*, 209-216. 10.1097/01.pra.0000386907.99536.75.

45. Takahashi, K., Tanabe, K., Ohnuki, M., Narita, M., Sasaki, A., Yamamoto, M., Nakamura, M., Sutou, K., Osafune, K., and Yamanaka, S. (2014). Induction of pluripotency in human somatic cells via a transient state resembling primitive streak-like mesendoderm. Nat Commun *5*, 3678. 10.1038/ncomms4678.

46. Ohnuki, M., Tanabe, K., Sutou, K., Teramoto, I., Sawamura, Y., Narita, M., Nakamura, M., Tokunaga, Y., Nakamura, M., Watanabe, A., et al. (2014). Dynamic regulation of human endogenous retroviruses mediates factor-induced reprogramming and differentiation potential. Proc Natl Acad Sci U S A *111*, 12426-12431. 10.1073/pnas.1413299111.

47. Karch, C.M., Kao, A.W., Karydas, A., Onanuga, K., Martinez, R., Argouarch, A., Wang, C., Huang, C., Sohn, P.D., Bowles, K.R., et al. (2019). A Comprehensive Resource for Induced Pluripotent Stem Cells from Patients with Primary Tauopathies. Stem Cell Reports *13*, 939-955. 10.1016/j.stemcr.2019.09.006.

48. Israel, M.A., Yuan, S.H., Bardy, C., Reyna, S.M., Mu, Y., Herrera, C., Hefferan, M.P., Van Gorp, S., Nazor, K.L., Boscolo, F.S., et al. (2012). Probing sporadic and familial Alzheimer's disease using induced pluripotent stem cells. Nature *482*, 216-220. 10.1038/nature10821.

49. Choi, S.H., Kim, Y.H., Hebisch, M., Sliwinski, C., Lee, S., D'Avanzo, C., Chen, H., Hooli, B., Asselin, C., Muffat, J., et al. (2014). A three-dimensional human neural cell culture model of Alzheimer's disease. Nature *515*, 274-278. 10.1038/nature13800.

50. Puigdevall, P., Jerber, J., Danecek, P., Castellano, S., and Kilpinen, H. (2023). Somatic mutations alter the differentiation outcomes of iPSC-derived neurons. Cell Genom *3*, 100280. 10.1016/j.xgen.2023.100280.

51. Osafune, K., Caron, L., Borowiak, M., Martinez, R.J., Fitz-Gerald, C.S., Sato, Y., Cowan, C.A., Chien, K.R., and Melton, D.A. (2008). Marked differences in differentiation propensity among human embryonic stem cell lines. Nat Biotechnol *26*, 313-315. 10.1038/nbt1383.

52. Huangfu, D., Osafune, K., Maehr, R., Guo, W., Eijkelenboom, A., Chen, S., Muhlestein, W., and Melton, D.A. (2008). Induction of pluripotent stem cells from primary human fibroblasts with only Oct4 and Sox2. Nat Biotechnol *26*, 1269-1275. 10.1038/nbt.1502.

53. De Paola, M., Pischiutta, F., Comolli, D., Mariani, A., Kelk, J., Lisi, I., Cerovic, M., Fumagalli, S., Forloni, G., and Zanier, E.R. (2023). Neural cortical organoids from self-assembling human iPSC as a model to investigate neurotoxicity in brain ischemia. J Cereb Blood Flow Metab *43*, 680-693. 10.1177/0271678X231152023.

54. Gabriel, E., and Gopalakrishnan, J. (2017). Generation of iPSC-derived Human Brain Organoids to Model Early Neurodevelopmental Disorders. J Vis Exp. 10.3791/55372.

55. Hirt, C.K., Booij, T.H., Grob, L., Simmler, P., Toussaint, N.C., Keller, D., Taube, D., Ludwig, V., Goryachkin, A., Pauli, C., et al. (2022). Drug screening and genome editing in human pancreatic cancer organoids identifies drug-gene interactions and candidates for off-label treatment. Cell Genom *2*, 100095. 10.1016/j.xgen.2022.100095.

56. Chen, C., Ji, W., and Niu, Y. (2021). Primate Organoids and Gene-Editing Technologies toward Next-Generation Biomedical Research. Trends Biotechnol *39*, 1332-1342. 10.1016/j.tibtech.2021.03.010.

57. Zhou, H., Wang, Y., Liu, L.P., Li, Y.M., and Zheng, Y.W. (2021). Gene Editing in Pluripotent Stem Cells and Their Derived Organoids. Stem Cells Int *2021*, 8130828. 10.1155/2021/8130828.

656   58. Kelava, I., and Lancaster, M.A. (2016). Stem Cell Models of Human Brain Development. Cell Stem
657   Cell *18*, 736-748. 10.1016/j.stem.2016.05.022.

658   59. Kelava, I., and Lancaster, M.A. (2016). Dishing out mini-brains: Current progress and future
659   prospects in brain organoid research. Dev Biol *420*, 199-209. 10.1016/j.ydbio.2016.06.037.

660   60. Ham, O., Jin, Y.B., Kim, J., and Lee, M.O. (2020). Blood vessel formation in cerebral organoids
661   formed from human embryonic stem cells. Biochem Biophys Res Commun *521*, 84-90.
662   10.1016/j.bbrc.2019.10.079.

663   61. Tirughana, R., Metz, M.Z., Li, Z., Hall, C., Hsu, D., Beltzer, J., Annala, A.J., Oganesyan, D., Gutova,
664   M., and Aboody, K.S. (2018). GMP Production and Scale-Up of Adherent Neural Stem Cells with a
665   Quantum Cell Expansion System. Mol Ther Methods Clin Dev *10*, 48-56.
666   10.1016/j.omtm.2018.05.006.

667   62. Hubert, C.G., Rivera, M., Spangler, L.C., Wu, Q., Mack, S.C., Prager, B.C., Couce, M., McLendon,
668   R.E., Sloan, A.E., and Rich, J.N. (2016). A Three-Dimensional Organoid Culture System Derived
669   from Human Glioblastomas Recapitulates the Hypoxic Gradients and Cancer Stem Cell
670   Heterogeneity of Tumors Found In Vivo. Cancer Res *76*, 2465-2477. 10.1158/0008-5472.CAN-15-
671   2402.

672   63. Lancaster, M.A., and Knoblich, J.A. (2014). Generation of cerebral organoids from human
673   pluripotent stem cells. Nat Protoc *9*, 2329-2340. 10.1038/nprot.2014.158.

674   64. Ashburner, M., Ball, C.A., Blake, J.A., Botstein, D., Butler, H., Cherry, J.M., Davis, A.P., Dolinski,
675   K., Dwight, S.S., Eppig, J.T., et al. (2000). Gene ontology: tool for the unification of biology. The
676   Gene Ontology Consortium. Nat Genet *25*, 25-29. 10.1038/75556.

677   65. Gene Ontology, C., Aleksander, S.A., Balhoff, J., Carbon, S., Cherry, J.M., Drabkin, H.J., Ebert, D.,
678   Feuermann, M., Gaudet, P., Harris, N.L., et al. (2023). The Gene Ontology knowledgebase in 2023.
679   Genetics *224*. 10.1093/genetics/iyad031.

680   66. Thomas, P.D., Ebert, D., Muruganujan, A., Mushayahama, T., Albou, L.P., and Mi, H. (2022).
681   PANTHER: Making genome-scale phylogenetics accessible to all. Protein Sci *31*, 8-22.
682   10.1002/pro.4218.

683
684

685   **FIGURE LEGENDS**

686

687   **Figure 1. LMNSC01 organoid growth, maturation, and layer formation.**

688   **(A)** Brightfield images of LMNSC01 organoids from an initial seed of 1000 cells/organoid (D0).

689   Organoids progressively increase in confluency between D0 and D47. At D15 the organoids appear more

690   homogeneous; internal structure becomes evident at D30.

691   **(B)** Reconstructed confocal images of enhanced green fluorescent protein (eGFP)-expressing LMNSC01

692   cells illustrating expansion, folding, and internal architectural complexity that becomes evident at D30.

693   Some organoids curl (D60), while most remain roughly spherical (D90).

694   **(C)** Increase in numbers of cells per organoid over 120 days in culture: rapid growth over the first 30

695   days, a characteristic dip at D60, followed by stabilization at D90 to D120 (*: $p < 0.05$; **: $p < 0.01$;

696   ****: $p < 0.001$). Organoids were dissociated, and cells counted by flow cytometry. Cell viability after

697   organoid dissociation: D15, $96.6 \pm 1.0\%$; D30, $92.0 \pm 2.6\%$; D60, $88.2 \pm 2.4\%$; D90, $95.2 \pm 0.3\%$; D120,

698    $91.4 \pm 0.5\%$ (mean ± s.d., number of organoids as indicated on the figure).

699   **(D)** Eccentricity of organoid shape assessed as major axis/minor axis, illustrating that most organoids

700   were smooth and ovoid (green bars). Grey bars denote organoids identified by eye as not smoothly

701   spherical or ovoid. By this measure, 1.0 indicates a spherical organoid. Numbers of organoids are as

702   indicated on the figure. The majority of organoids were smooth spherical/ovoid: D15, 66%; D30, 94%,

703   D60, 100%, D90, 82%. Statistical tests are between smooth/ovoid populations.

704   **(E)** Organoid cross-sectional areas over time in culture. This value remained relatively stable at around 2

705   mm^2 for both spherical/ovoid and more eccentric organoids. Mean diameters measured as average of

706   major and minor axis (mm): D15, 1.7 ± 0.2; D30, 1.6 ± 0.4; D60, 1.6 ± 0.4; D90, 1.3 ± 0.1 (mean ± s.d.);

707    $p < 0.05$ for all days relative to D90, all other comparisons not significant; numbers of organoids as

708   indicated on the figure.

709   **(F)** Expression (NanoString) of genes in the pathway "Tissue Integrity and Maintenance" (**Supplemental**

710   **Table 1**), ordered by expression level at D120. **(i)** Genes that show their highest expression at D30, and

711   whose expression becomes minimal at D120 (blue time arrow). **(ii)** Genes with higher expression in

712   organoids between D34-D120 and whose expression is maintained at D120.

713   **(G)** D30 organoid. Series of images of organoid edge at increasing depth (schematic), as described in the

714   text, showing stratification of GFAP[POS], SOX2[POS], and β-tubulin III[POS] cells.

715   **(H)** D30 organoid. Neurons (NeuN^{POS} and MAP2^{POS}) are internal to GFAP^{POS} glia near the organoid

716   surface.

717   **(I)** D30 organoid. PAX6^{POS} cortically fated cells surrounding a ventricle-like cell-free area, internal to a

718   surround of β-tubulin III^{POS} immature neurons.

719

Figure 2. LM-NSC008 organoids express markers indicative of a telencephalon (cortical and hippocampal) identity.

(A1) 3D reconstruction of organoid immunofluorescence; SOX2-expressing stem and progenitor cells remain distributed throughout organoids over the period D15-D90.

(A2) Percentage of SOX2^{POS} cells over the *in vitro* period (D15-D120), as measured by organoid dissociation and flow cytometry. *: $p < 0.05$, n = 4 at each time point.

(B,C) Paired images of entire organoids (3D reconstruction, above) and detail (single optical section, below).

(B) FoxG1 immunofluorescence marking forebrain-fated cortical progenitor cells.

(C) Persistence of Wnt receptor Fdz9, a marker of hippocampal fate, D30-D90, also illustrating changes in cell morphology.

(D) Expression of TTR (a marker of choroid plexus fate) by immunofluorescence. D30 organoid.

(E) Heatmap of cell type clustering by expression profiling within fetal cortex (BrainSpan, in weeks post-conception) and organoids (NanoString, in weeks *in vitro*).

(F) Dendrogram constructed from NanoString expression profiling of cell type markers (from **E**), indicating the closest relatedness of organoids to cortex and distance from other regions.

Figure 3. Progression of neuronal differentiation marker expression over time.

Diagonal lines indicate image or data not available.

(A1-E1) Immunofluorescence image pairs of representative organoids. Above, confocal 3D reconstructions of entire organoids; below, detailed higher resolution single optical sections (below).

(A2-E2) Expression of markers, by percentage of total positive cells (by dissociation and flow cytometry; blue), and by mRNA levels in organoids (NanoString; red) and fetal cortex (BrainSpan; black). Data are plotted at 70% transparency; the inset illustrates increasing density of dots with overlap of multiple points.

(A2) Transcription factor T-box brain1 (Tbr1), a marker of postmitotic neurons [17], see text.

(B1, B2) Doublecortin (DCX), a marker of migrating early neurons, see text.

(C1, C2) β-Tubulin III, a marker of maturing neurons [19]; see text.

(D1, D2) MAP2, a neural differentiation marker [20]; see text

(E1, E2) NeuN, a nuclear marker of mature neurons [21]; see text.

751 **Figure 4. Differentiation of macroglia (astrocytes and oligodendrocytes) in organoids over time.**

752 *In this figure, each dot represents a data point from an organoid (NanoString) or a cortical specimen*

753 *(BrainSpan). The horizontal lines indicate the mean of the data. The lines are included to aid in viewing*

754 *trends in the data.*

755 **(A)** Expression of SOX9 by immunofluorescence, often in the nuclei of vimentin-expressing

756 neuroprogenitor cells (white arrow heads).

757 **(B)** Expression of oligodendrocyte marker O1 by immunofluorescence.

758 **[C]** Expression of phospho-vimentin in cell bodies of mitotic GFAP-expressing cells by

759 immunofluorescence.

760 **(Da, i-iii)** Maintained expression of SOX9 in organoids of increasing age by immunofluorescence.

761 **(Da, iv-vi)** Expression of GFAP in organoids of increasing age by immunofluorescence.

762 **(Db)** Almost parallel expression of GFAP as percent expressing cells (flow cytometry) and mRNA

763 (NanoString), with a transient decrease around D60.

764 **(Dc)** Expression of SOX9 mRNA in organoids (red, NanoString) and fetal cortex (black, BrainSpan).

765 **(Dd)** Expression of GFAP mRNA in organoids (red, NanoString) and fetal cortex (black, BrainSpan).

766 Numbers of organoids expression profiled by NanoString for days in culture (D); numbers of

767 organoids/number of cohorts: D34, 4/1; D60, 10/2; D65, 4/1; D90, 7/2; D94, 4/1; D120, 4/1.

768 Numbers of cortical region fetal samples as reported by BrainSpan for weeks post-conception (W);

769 numbers of samples/number of donors: W8, 9/1; W9, 7/1; W12, 31/3; W13, 32/3; W16, 28/3; W17, 9/1;

770 W19, 8/1; W21, 11/2; W24, 11/1; W25, 1/1; W26, 3/1; W35, 1/1; W37, 11/1.

771

772 **Figure 5. Immunostained LMNSC01 organoids express endothelial markers CD31 and von**

773 **Willebrand Factor (vWF), and the tight junction protein ZO-1.**

774 Yellow arrowheads indicate alignment of these markers in linear arrangements suggestive of nascent

775 vasculature, increasing in older organoids.

776

777

778 **Figure 6. Progression of developmental programs in organoids and during fetal cortical**

779 **development.**

780 **(A1)** Cross correlation for expression of the genes in the NanoString Human Neuropathology Panel

781 (**Supplemental Table S1**) by each of 33 organoids ranging from D34 to D120 in culture, illustrating the

782 similarities in gene expression between organoids of similar ages, and pronounced differences with

783 organoids of different ages.

784 **(A2)** Similar cross correlation for the same genes during normal fetal development drawn from the

785 BrainSpan database.

786 **(B)** *Singscores*, expression relative to NanoString-defined reference genes, where 0.5 indicates no

787 difference, over time for three major NSC-lineage cell types in organoids (top, red) and fetal cortex

788 (middle, black). Below are the same data plotted on a relative time scale, 0.0-1.0, for organoids (D0-D120

789 in culture) and fetal cortex (W0-W37 post-conception, W40 marks full human gestation). These plots

790 illustrate the quantitative similarities between organoids and fetal cortex for both expression levels and

791 waveforms.

792 **(C)** Similar data for seven themes and pathways (**Supplementary Table S1**); the complete data are shown

793 in **Supplemental Figure S2**.

794

795

796   **Figure 7. Growth conditions alter LMNSC01 organoid differentiation.**

797   **A,** Experimental schema. Organoids were initially grown (4% O_2) in NeuroCult (NC) Proliferation

798   medium until D15, then optionally transferred to NC Differentiation medium until D30 or longer. P = NC

799   Proliferation medium. D = NC Differentiation medium. n = numbers of organoids as indicated.

800   **B,** Numbers of cells per organoid (*above*) after D15 continued to increase in NC Proliferation medium

801   (EGF and FGF supplemented) (blue line), but stabilized in NC Differentiation medium (no added

802   EGF/FGF) (red line). Organoid diameters (*below*), averages of major and minor axes, were relatively

803   independent of growth medium.

804   **C,** Maturation of neuron morphology and apparent synaptogenesis at D30 in NC Differentiation medium.

805   **i,** Neuronal processes, marked by β-tubulin III expression, were extended and smooth in NC Proliferation

806   medium. **ii,** Neuronal varicosities developed in NC Differentiation medium. **iii,** Varicosities (MAP2[POS])

807   also express synapsin1.

808   **D,** At D104, GFAP[POS] astrocytes extended processes and formed bundles in NC Differentiation medium.

809   **E,** Organoids grown in NC Differentiation medium from D15: O1[POS] oligodendrocyte cells extended

810   process by D30, and by D104 became highly ramified.
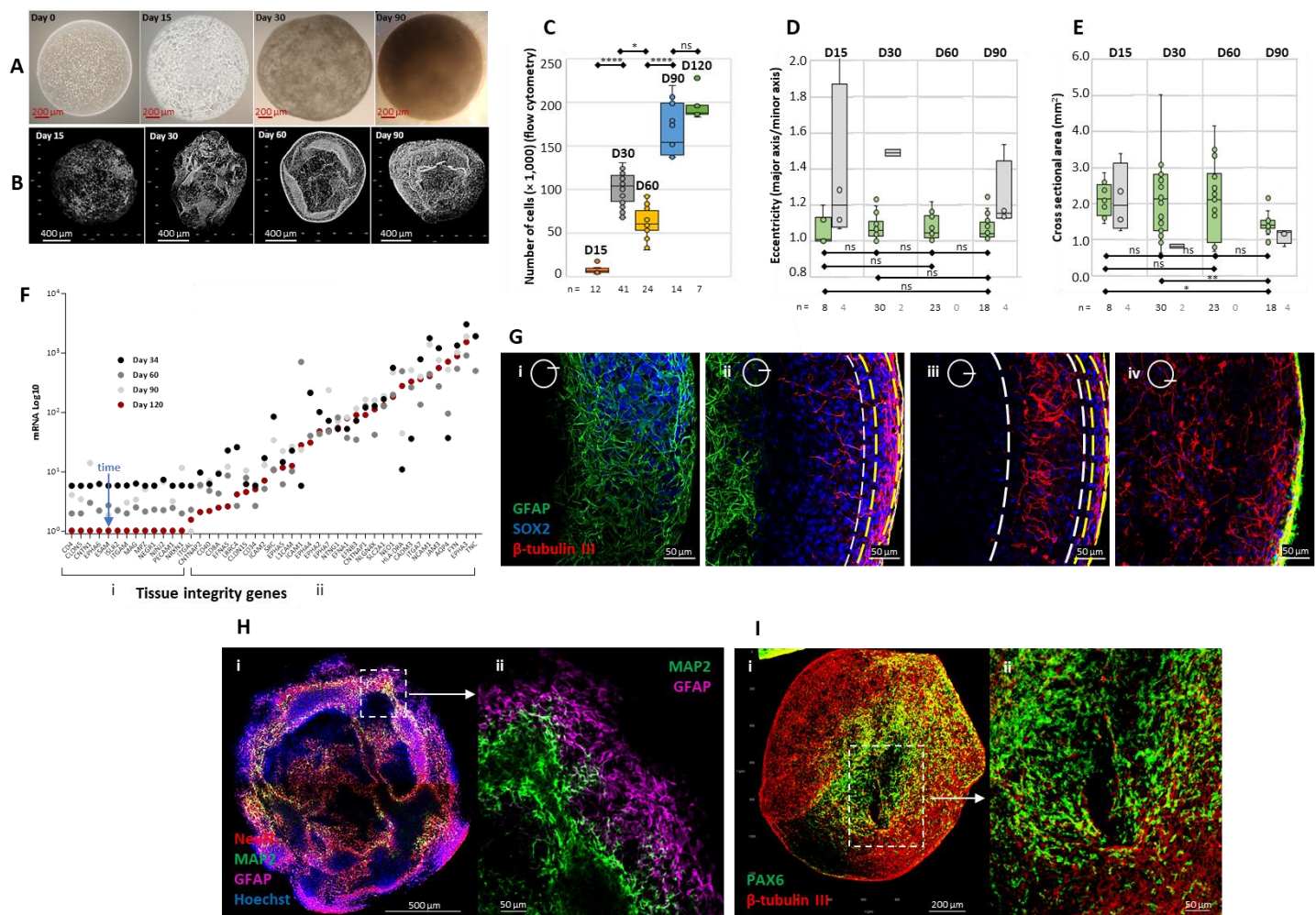
811

Figure 1. LMNSC01 organoid growth, maturation, and layer formation.

(A) Brightfield images of LMNSC01 organoids from an initial seed of 1000 cells/organoid (D0). Organoids progressively increase in confluency between D0 and D47. At D15 the organoids appear more homogeneous; internal structure becomes evident at D30.

(B) Reconstructed confocal images of enhanced green fluorescent protein (eGFP)-expressing LMNSC01 cells illustrating expansion, folding, and internal architectural complexity that becomes evident at D30. Some organoids curl (D60), while most remain roughly spherical (D90).

(C) Increase in numbers of cells per organoid over 120 days in culture: rapid growth over the first 30 days, a characteristic dip at D60, followed by stabilization at D90 to D120 (*: $p < 0.05$; **: $p < 0.01$; ****: $p < 0.001$). Organoids were dissociated, and cells counted by flow cytometry. Cell viability after organoid dissociation: D15, 96.6 ± 1.0%; D30, 92.0 ± 2.6%; D60, 88.2 ± 2.4%; D90, 95.2 ± 0.3%; D120, 91.4 ± 0.5% (mean ± s.d., number of organoids as indicated on the figure).

(**D**) Eccentricity of organoid shape assessed as major axis/minor axis, illustrating that most organoids were smooth and ovoid (green bars). Grey bars denote organoids identified by eye as not smoothly spherical or ovoid. By this measure, 1.0 indicates a spherical organoid. Numbers of organoids are as indicated on the figure. The majority of organoids were smooth spherical/ovoid: D15, 66%; D30, 94%, D60, 100%, D90, 82%. Statistical tests are between smooth/ovoid populations.

(**E**) Organoid cross-sectional areas over time in culture. This value remained relatively stable at around 2 mm^2 for both spherical/ovoid and more eccentric organoids. Mean diameters measured as average of major and minor axis (mm): D15, 1.7 ± 0.2; D30, 1.6 ± 0.4; D60, 1.6 ± 0.4; D90, 1.3 ± 0.1 (mean ± s.d.); p < 0.05 for all days relative to D90, all other comparisons not significant; numbers of organoids as indicated on the figure.

(**F**) Expression (NanoString) of genes in the pathway "Tissue Integrity and Maintenance" (**Supplemental Table 1**), ordered by expression level at D120. (**i**) Genes that show their highest expression at D30, and whose expression becomes minimal at D120 (blue time arrow). (**ii**) Genes with higher expression in organoids between D34-D120 and whose expression is maintained at D120.

(**G**) D30 organoid. Series of images of organoid edge at increasing depth (schematic), as described in the text, showing stratification of GFAP^{POS}, SOX2^{POS}, and β-tubulin III^{POS} cells.

(**H**) D30 organoid. Neurons (NeuN^{POS} and MAP2^{POS}) are internal to GFAP^{POS} glia near the organoid surface.

(**I**) D30 organoid. PAX6^{POS} cortically fated cells surrounding a ventricle-like cell-free area, internal to a surround of β-tubulin III^{POS} immature neurons.
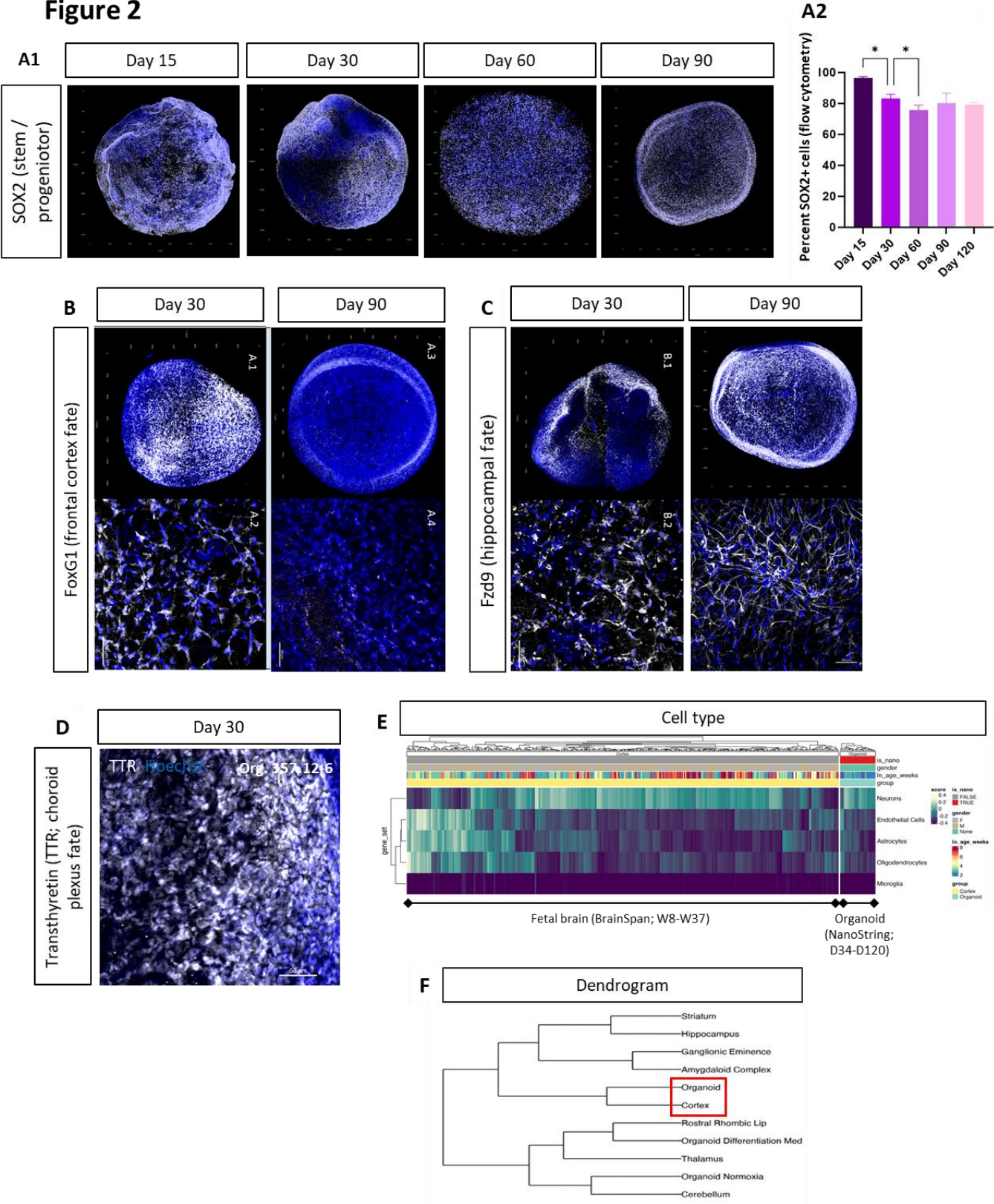
Figure 2

Figure 2. LM-NSC008 organoids express markers indicative of a telencephalon (cortical and hippocampal) identity.

(A1) 3D reconstruction of organoid immunofluorescence; SOX2-expressing stem and progenitor cells remain distributed throughout organoids over the period D15-D90.

(A2) Percentage of SOX2^{POS} cells over the *in vitro* period (D15-D120), as measured by organoid dissociation and flow cytometry. *: $p < 0.05$, n = 4 at each time point.

(B,C) Paired images of entire organoids (3D reconstruction, above) and detail (single optical section, below).

(B) FoxG1 immunofluorescence marking forebrain-fated cortical progenitor cells.

(C) Persistence of Wnt receptor Fdz9, a marker of hippocampal fate, D30-D90, also illustrating changes in cell morphology.

(D) Expression of TTR (a marker of choroid plexus fate) by immunofluorescence. D30 organoid.

(E) Heatmap of cell type clustering by expression profiling within fetal cortex (BrainSpan, in weeks post-conception) and organoids (NanoString, in weeks *in vitro*).

(F) Dendrogram constructed from NanoString expression profiling of cell type markers (from **E**), indicating the closest relatedness of organoids to cortex and distance from other regions.
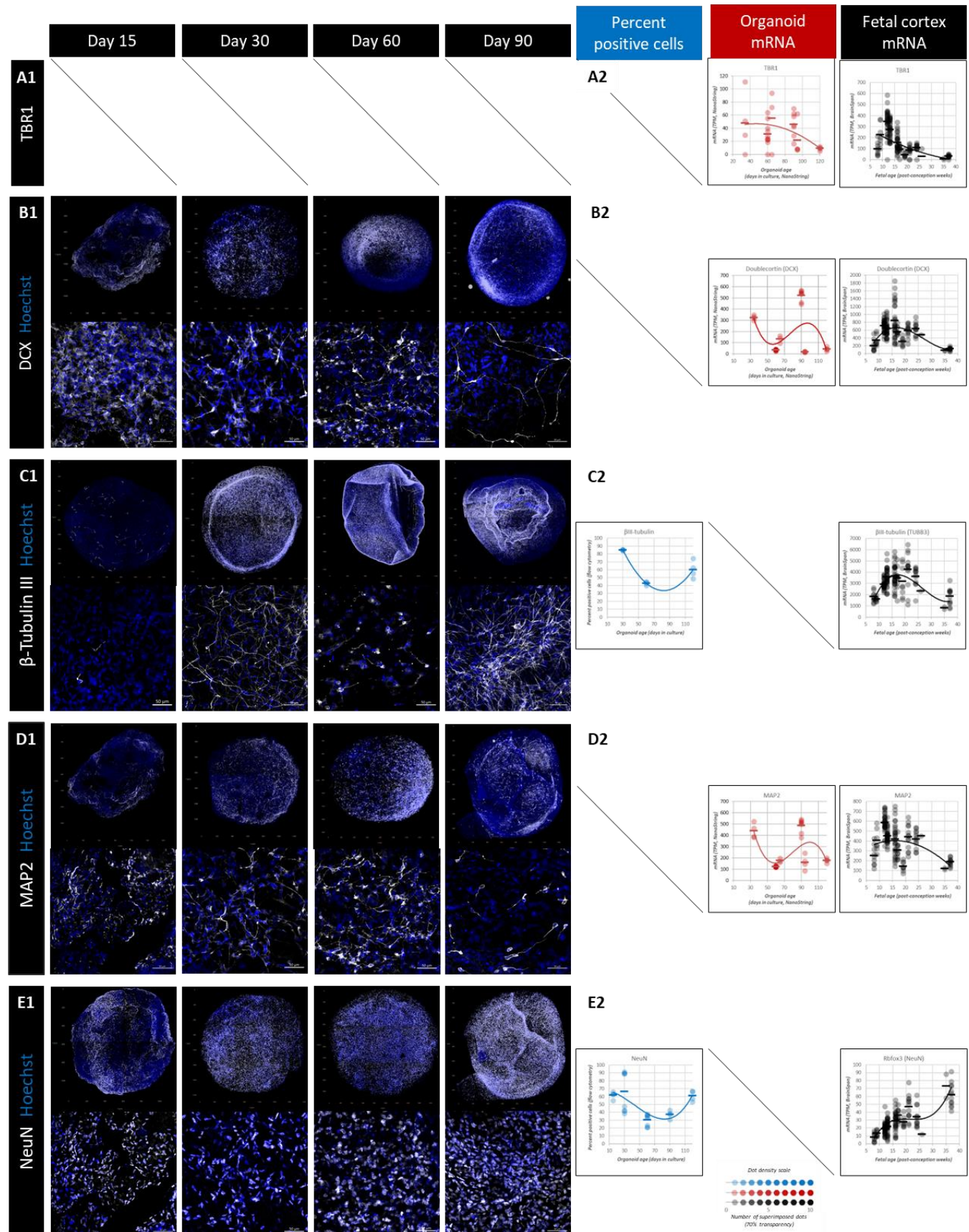
Figure 3. Progression of neuronal differentiation marker expression over time.

Diagonal lines indicate image or data not available.

(A1-E1) Immunofluorescence image pairs of representative organoids. Above, confocal 3D reconstructions of entire organoids; below, detailed higher resolution single optical sections (below).

(A2-E2) Expression of markers, by percentage of total positive cells (by dissociation and flow cytometry; blue), and by mRNA levels in organoids (NanoString; red) and fetal cortex (BrainSpan; black). Data are plotted at 70% transparency; the inset illustrates increasing density of dots with overlap of multiple points.
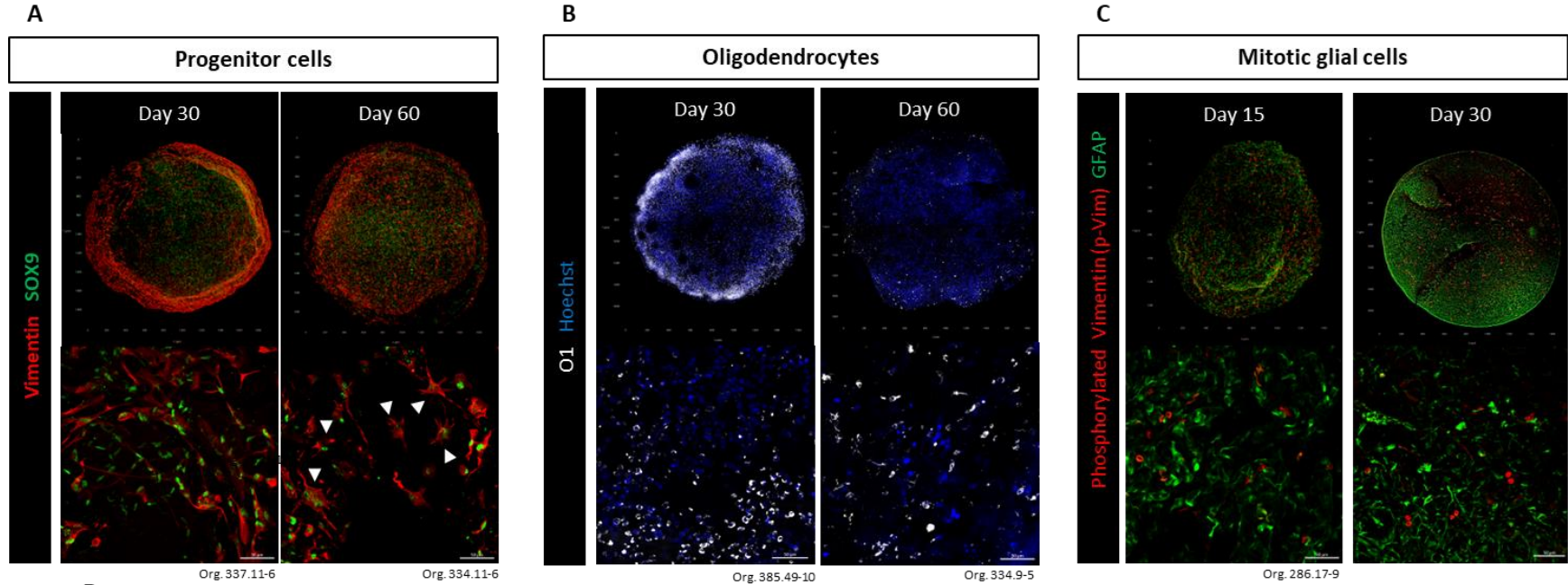
(A2) Transcription factor T-box brain1 (Tbr1), a marker of postmitotic neurons [31], see text.

(B1, B2) Doublecortin (DCX), a marker of migrating early neurons, see text.

(C1, C2) β-Tubulin III, a marker of maturing neurons [33]; see text.

(D1, D2) MAP2, a neural differentiation marker [34]; see text

(E1, E2) NeuN, a nuclear marker of mature neurons [35]; see text.

A Progenitor cells

Day 30 | Day 60

Vimentin | SOX9

Org. 337.11-6 | Org. 334.11-6

B Oligodendrocytes

Day 30 | Day 60

O1 | Hoechst

Org. 385.49-10 | Org. 334.9-5

C Mitotic glial cells

Day 15 | Day 30

Phosphorylated Vimentin (p-Vim) | GFAP

Org. 286.17-9

D Astrocytes

a

Day 15 | Day 30 | Day 60

i | ii | iii

SOX9 Hoechst | SOX9 Hoechst | SOX9 Hoechst

iv | v | vi

GFAP | GFAP | GFAP

b GFAP

Percent positive cells (flow cytometry) / mRNA (TPM, NanoString)

Organoid age (days in culture)

c SOX9

mRNA (TPM, NanoString) — Organoid age (days in culture, NanoString)

SOX9

mRNA (TPM, BrainSpan) — Fetal age (post-conception weeks)

d GFAP

mRNA (TPM, NanoString) — Organoid age (days in culture, NanoString)

GFAP

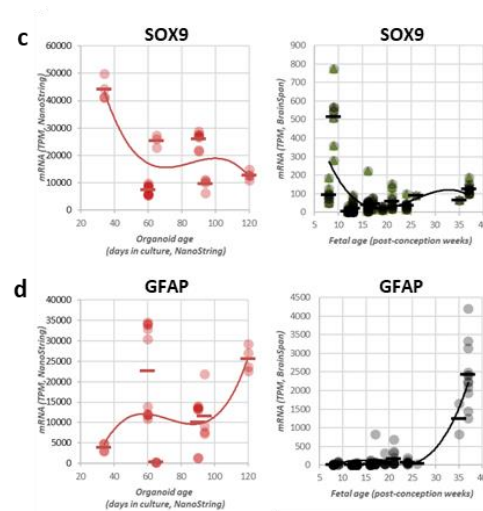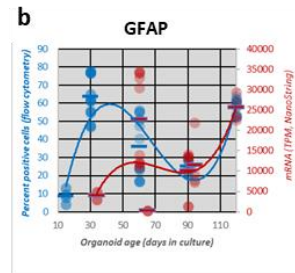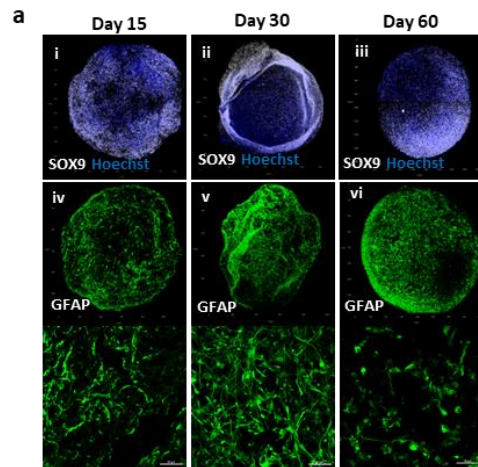mRNA (TPM, BrainSpan) — Fetal age (post-conception weeks)

Figure 4. Differentiation of macroglia (astrocytes and oligodendrocytes) in organoids over time.

In this figure, each dot represents a data point from an organoid (NanoString) or a cortical specimen (BrainSpan). The horizontal lines indicate the mean of the data. The lines are included to aid in viewing trends in the data.

(A) Expression of SOX9 by immunofluorescence, often in the nuclei of vimentin-expressing neuroprogenitor cells (white arrow heads).

(B) Expression of oligodendrocyte marker O1 by immunofluorescence.

[C] Expression of phospho-vimentin in cell bodies of mitotic GFAP-expressing cells by immunofluorescence.

(Da, i-iii) Maintained expression of SOX9 in organoids of increasing age by immunofluorescence.

(Da, iv-vi) Expression of GFAP in organoids of increasing age by immunofluorescence.

(Db) Almost parallel expression of GFAP as percent expressing cells (flow cytometry) and mRNA (NanoString), with a transient decrease around D60.

(Dc) Expression of SOX9 mRNA in organoids (red, NanoString) and fetal cortex (black, BrainSpan).

(Dd) Expression of GFAP mRNA in organoids (red, NanoString) and fetal cortex (black, BrainSpan).

Numbers of organoids expression profiled by NanoString for days in culture (D); numbers of organoids/number of cohorts: D34, 4/1; D60, 10/2; D65, 4/1; D90, 7/2; D94, 4/1; D120, 4/1.

Numbers of cortical region fetal samples as reported by BrainSpan for weeks post-conception (W); numbers of samples/number of donors: W8, 9/1; W9, 7/1; W12, 31/3; W13, 32/3; W16, 28/3; W17, 9/1; W19, 8/1; W21, 11/2; W24, 11/1; W25, 1/1; W26, 3/1; W35, 1/1; W37, 11/1.
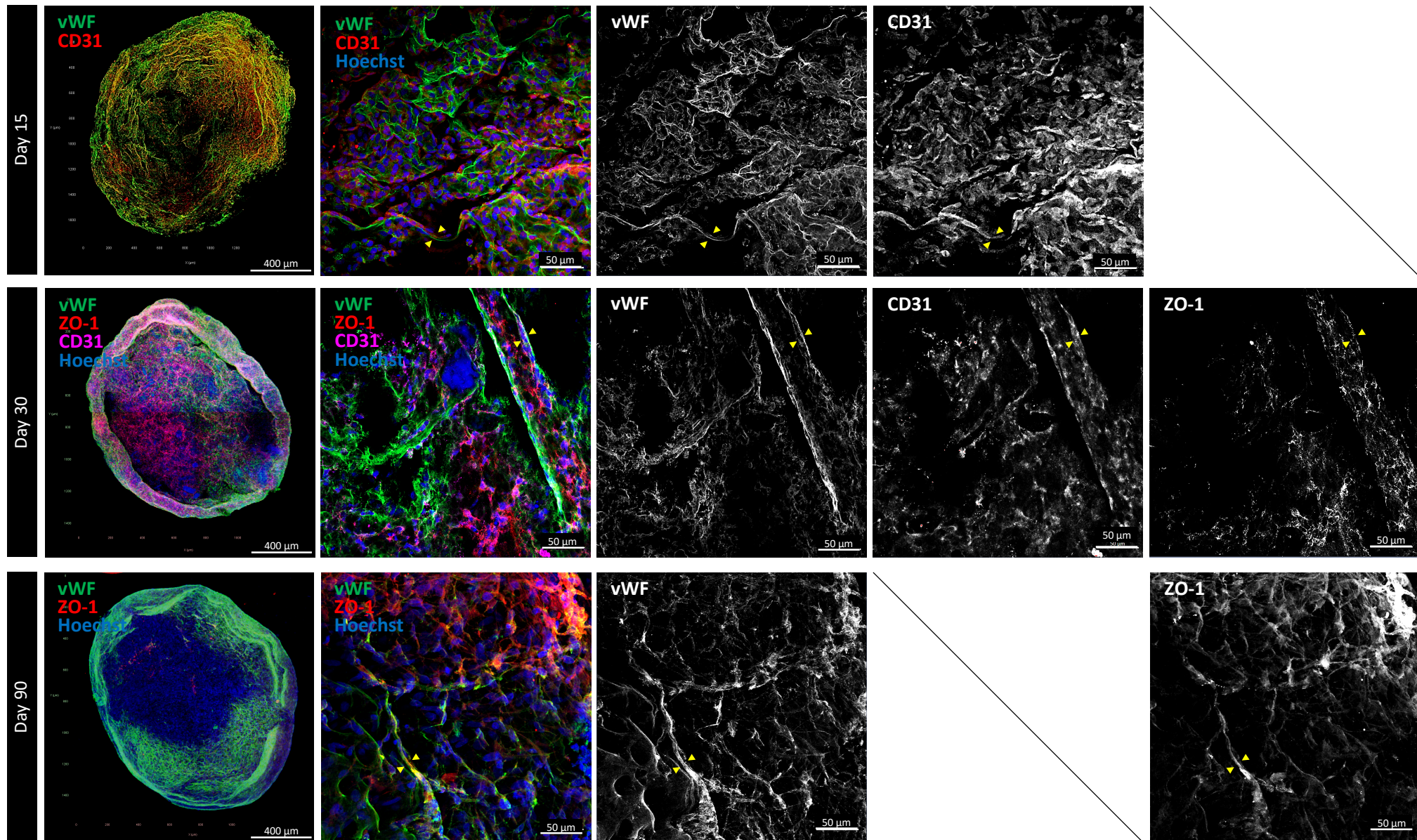
Figure 5. Immunostained LMNSC01 organoids express endothelial markers CD31 and von Willebrand Factor (vWF), and the tight junction protein ZO-1.

Yellow arrowheads indicate alignment of these markers in linear arrangements suggestive of nascent vasculature, increasing in older organoids.
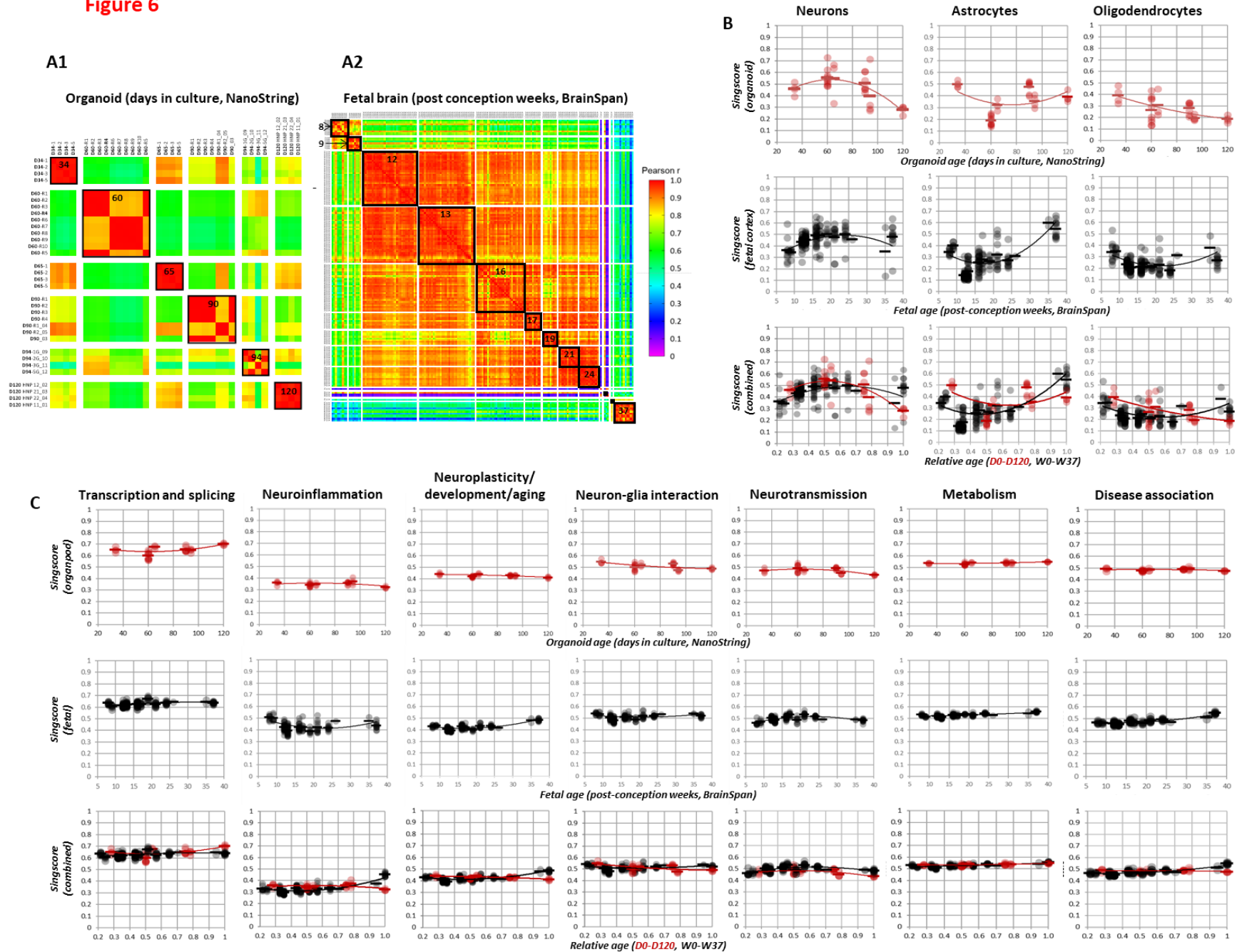
Figure 6

Figure 6. Progression of developmental programs in organoids and during fetal cortical development.

(A1) Cross correlation for expression of the genes in the NanoString <mark>Neuroinflammation</mark> panel (**Supplemental Table S1**) by each of 33 organoids ranging from D34 to D120 in culture, illustrating the similarities in gene expression between organoids of similar ages, and pronounced differences with organoids of different ages.

(A2) Similar cross correlation for the same genes during normal fetal development drawn from the BrainSpan database.

(B) *Singscores*, expression relative to NanoString-defined reference genes, where 0.5 indicates no difference, over time for three major NSC-lineage cell types in organoids (top, red) and fetal cortex (middle, black). Below are the same data plotted on a relative time scale, 0.0-1.0, for organoids (D0-D120 in culture) and fetal cortex (W0-W37 post-conception, W40 marks full human gestation). These plots illustrate the quantitative similarities between organoids and fetal cortex for both expression levels and waveforms.

(C) Similar data for seven themes and pathways (**Supplementary Table S1**); the complete data are shown in **Supplemental Figure S2**.
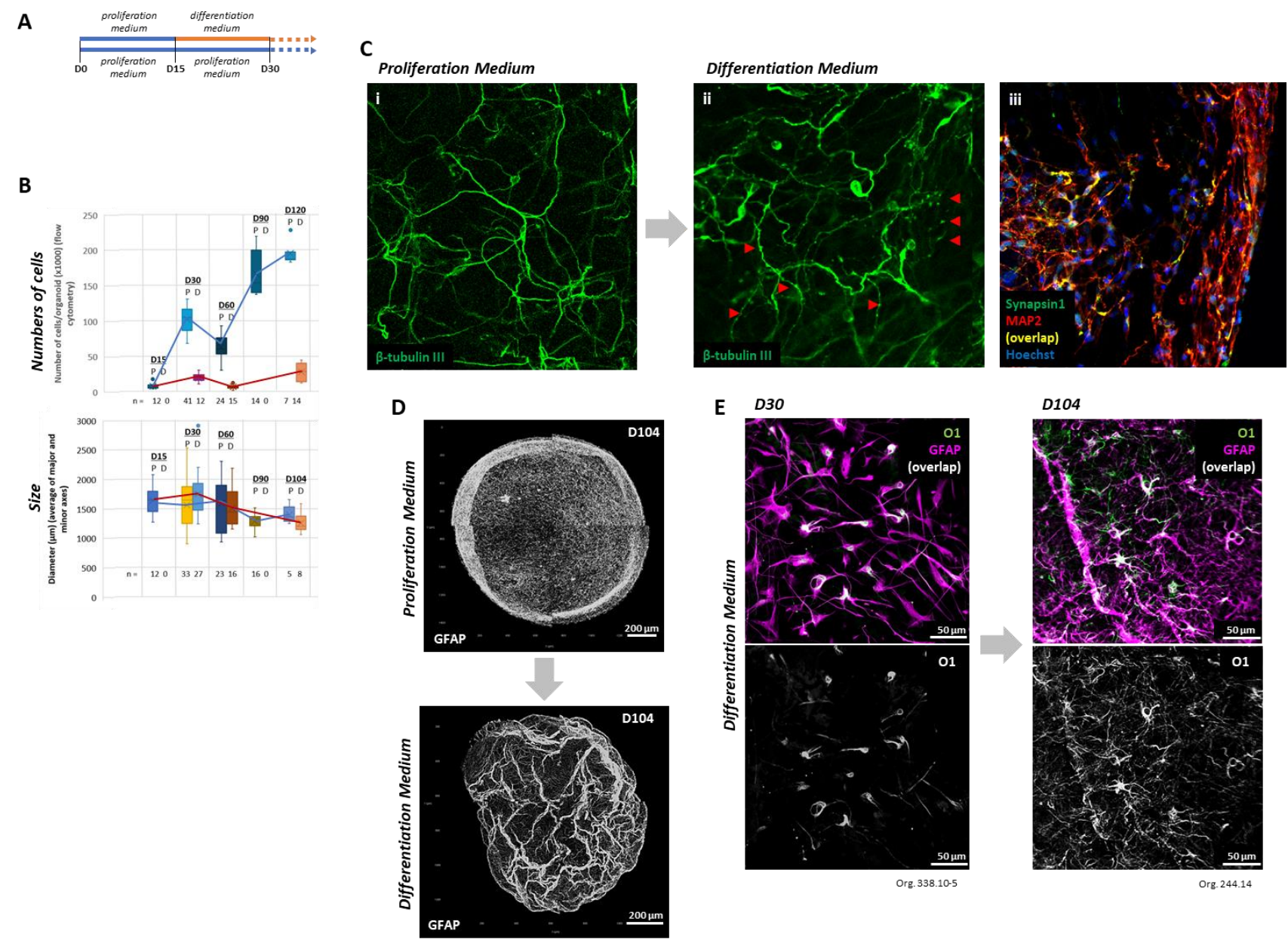
Figure 7. Transition to differentiation medium

A

proliferation medium / differentiation medium

D0 — D15 — D30

B *Numbers of cells* / *Size*

C

Proliferation Medium — *Differentiation Medium*

i β-tubulin III

ii β-tubulin III

iii Synapsin1 / MAP2 / (overlap) / Hoechst

D *Proliferation Medium* / *Differentiation Medium* — GFAP — D104 — 200 µm

E D30 — D104 — O1 / GFAP (overlap) — O1 — 50 µm — *Differentiation Medium*

Org. 338.10-5 — Org. 244.14

Figure 7. Growth conditions alter LMNSC01 organoid differentiation.

A, Experimental schema. Organoids were initially grown (4% O2) in NeuroCult (NC) Proliferation medium until D15, then optionally transferred to NC Differentiation medium until D30 or longer. P = NC Proliferation medium. D = NC Differentiation medium. n = numbers of organoids as indicated.

B, Numbers of cells per organoid (*above*) after D15 continued to increase in NC Proliferation medium (EGF and FGF supplemented) (blue line), but stabilized in NC Differentiation medium (no added EGF/FGF) (red line). Organoid diameters (*below*), averages of major and minor axes, were relatively independent of growth medium.

C, Maturation of neuron morphology and apparent synaptogenesis at D30 in NC Differentiation medium. **i,** Neuronal processes, marked by β-tubulin III expression, were extended and smooth in NC Proliferation medium. **ii**, Neuronal varicosities developed in NC Differentiation medium. **iii,** Varicosities (MAP2^{POS}) also express synapsin1.

D, At D104, GFAP^{POS} astrocytes extended processes and formed bundles in NC Differentiation medium.

E, Organoids grown in NC Differentiation medium from D15: O1^{POS} oligodendrocyte cells extended process by D30, and by D104 became highly ramified.